UNIVERSIDADE DE LISBOA
FACULDADE DE CIÊNCIAS
DEPARTAMENTO DE QUÍMICA E BIOQUÍMICA

# Exploring the role of the JAK3/STAT3 pathway in colorectal cancer

Catarina Sofia Ferreira Violante

**Mestrado em Bioquímica e Biomedicina**

Dissertação orientada por:
Dr. Federico Herrera
Dr. Sergio Alonso

2024

## Acknowledgements

As I complete this dissertation, I would like to extend my deepest gratitude to all those who contributed to the development of this work.

First and foremost, I wish to express my heartfelt thanks to Dr. Sergio Alonso and Dr. Beatriz Gonzalez for the invaluable opportunity to intern in their laboratory. Your unwavering support and warm welcome, both in and outside the lab, made my time in Badalona memorable. I will always cherish the sense of belonging you provided, and the experiences I had there will remain with me forever.

I am equally grateful to Dr. Federico Herrera for graciously welcoming me into his laboratory for the second part of my thesis and your relentless support while writing it.

To my colleagues in Cancer Genetics and Epigenetics, Carlos Mateos, Maria Navarro, and Anna Pujol, thank you for embracing me into your lab and making me feel like part of your little family. I will always remember our coffee runs, soaking up the sun, and the lively conversations we shared. A special mention goes to Paula Gonçalves, who sat across from me. You were an absolute delight to get to know, and I am grateful for the care you took to show me around.

To my colleagues in Cell Structure and Dynamics, Fernanda Murtinheira, Carina Coelho, Ana Sofia, Constança Pimenta, and Pedro Peralta, thank you for welcoming me with open arms, even though I joined in the middle of the year. I never felt like an outsider, and our shared love for coffee and snacks helped us forge a strong bond.

I would also like to thank the Erasmus+ Training Programme and my faculty for the scholarship that enabled me to spend such an enriching and fulfilling time at IGTP and in Barcelona. I am also grateful to the Cystic Fibrosis Research Lab at BioISI, especially to my colleague and friend Mariana Caleiro and Dr Margarida Gama-Carvalho at the RNA Systems Biology Lab (BioISI), for providing the cells needed for a positive control.

A special thank you goes to Dina and Luís, who treated me as one of their own during these two years of my master's journey. Your kindness and generosity were a constant source of comfort, and I will always be grateful. To my favourite person, Soraia Mestre, I truly could not have done this without you. You have been my greatest support, always encouraging me to follow my dreams and believe in myself, even when I found it difficult to do so. You were my home away from home, and for that, I am forever thankful.

To my lifelong friends, Catarina Moscoso, Joana Magalhães, and Sara Costa, as well as the friends I made later in life, Maria Macedo, Catarina São Pedro, and Patrícia Silvestre, thank you for the endless phone calls, check-ins, visits to Barcelona, and those simple yet precious coffee dates. Your presence made this journey lighter and much more enjoyable.

Lastly, I owe my deepest thanks to my parents for always supporting and believing in me from a young age, along with my brother Pedro, who in his own way has always supported and encouraged me. A special mention to my grandparents, whom I hope to make proud with this achievement.

## Abstract

Colorectal cancer (CRC) is one of the leading causes of cancer-related mortality worldwide. *Signal transducer and activator of transcription 3* (STAT3) is frequently dysregulated in various cancers, playing a pivotal role in tumour development and progression. Constitutive activation of STAT3 is observed in approximately 70% of solid tumours, highlighting its critical role in oncogenesis. Aberrant DNA methylation, a common epigenetic modification, occurs in nearly all CRC cases, prompting an investigation into the potential methylation of genes involved in the *STAT3* pathway, particularly its upstream regulators.

In this study, both in-house and publicly available CRC whole genome methylation databases were analysed to investigate *STAT3* promoter methylation, but this was not detected. The analysis was extended to all genes of the STAT3 pathway. The upstream effector *Janus kinase 3* (*JAK3*) was found to undergo promoter hypermethylation in a significant proportion of CRCs. The association between JAK*3* promoter methylation with gene expression was studied in a panel of 5 CRC cell lines. All the studied cell lines exhibited *JAK3* promoter methylation and low mRNA expression. Treatment with the inhibitor of methylation agent 5'-Aza-2′-deoxycytidine failed to restore gene transcription, indicating that promoter methylation is not the only factor underlying *JAK3* silencing. Further analysis examined JAK3 protein expression alongside phosphorylated STAT3 (pSTAT3) and total STAT3. JAK3 protein was undetectable in the 5 CRC cell lines. These findings underscore the complexity of signalling pathways involved in CRC and emphasize the necessity of further research to fully elucidate the mechanisms underlying STAT3 regulation and its role in colorectal oncogenesis.

**Keywords:** Colorectal cancer, STAT3, JAK3, DNA methylation, cancer cell lines

**Resumo**

O cancro colorretal (CRC) é o terceiro mais comum a nível mundial e a segunda principal causa de mortalidade por cancro. Na Península Ibérica, o CRC é o tipo de cancro mais frequentemente diagnosticado, uma tendência igualmente observada em muitos países em desenvolvimento. O CRC resulta da acumulação gradual de alterações genéticas e epigenéticas que transformam células epiteliais normais do cólon e do reto em adenocarcinomas invasivos. Entre as mutações genéticas mais comuns, destaca-se a inativação do gene *Adenomatous Polyposis Coli* (APC), que desregula a via de sinalização Wnt/β-catenina, responsável pela regulação da proliferação celular. Outras mutações relevantes ocorrem em genes supressores de tumores, como o *TP53*, e em proto oncogenes como *KRAS* e *BRAF*, sendo estas alterações fundamentais para a progressão do CRC.

Para além das mutações genéticas, as alterações epigenéticas, como a metilação do ADN, modificações das histonas e regulação por RNA não codificantes, desempenham um papel central na desenvolvimento e progressão do CRC. A metilação do ADN é uma das modificações epigenéticas mais estudadas e está frequentemente associada ao silenciamento transcricional de genes supressores de tumores. No CRC, são observadas alterações profundas no perfil de metilação do ADN, principalmente em regiões promotoras de genes críticos, o que afeta a sua expressão e promove a progressão do cancro.

Apesar dos avanços no tratamento do CRC, particularmente com a resseção cirúrgica e quimioterapia, desafios significativos persistem, sobretudo em casos metastáticos. Regimes de quimioterapia baseados no 5-fluorouracilo (5-FU), como FOLFOX e FOLFIRI, continuam a ser os principais tratamentos para estes casos, contribuindo para o prolongamento da sobrevivência dos pacientes. Adicionalmente, terapias direcionadas a vias de sinalização específicas, como EGFR e VEGF, têm demonstrado eficácia no controlo do crescimento tumoral e na prevenção de metástases. Mais recentemente, os inibidores de pontos de controlo imunitário (ICIs), como os que têm como alvo CTLA-4 e PD-1, revelaram-se promissores, especialmente em tumores com alta carga mutacional e forte infiltração de células imunitárias, conhecidos como tumores MSI-positivos (Instabilidade de Microssatélites). No entanto, a maioria dos tumores de CRC são MSS (Estabilidade de Microssatélites), sendo menos responsivos a estas imunoterapias, o que sublinha a necessidade de novas abordagens terapêuticas.

No contexto do CRC, uma área de investigação emergente é a via de sinalização *JAK-STAT* (*Janus kinase-Transdutor de Sinal e Ativador da Transcrição*), ativada por citocinas, fatores de crescimento e outros ligandos. Esta via regula funções celulares essenciais, incluindo o crescimento, a diferenciação e a resposta imunitária. A desregulação desta via, particularmente a ativação constitutiva de *STAT3*, está fortemente associada à promoção do crescimento tumoral e à evasão imunitária. Esta desregulação é observada em cerca de 70% dos tumores sólidos, tornando *STAT3* um alvo atrativo para intervenções terapêuticas no contexto oncológico.

O gene humano *Janus Kinase 3* (*JAK3*), localizado em 19p13.11, apresenta o padrão de expressão mais restrito entre os quatro genes *JAK*. É expresso principalmente em células hematopoiéticas pertencentes ao compartimento linfoide e em certas subpopulações de células mieloides, bem como em células endoteliais e mitóticas em órgãos hematopoiéticos e não hematopoiéticos. As mutações de perda de função na *JAK3* estão associadas a 5% dos casos de imunodeficiência combinada grave (SCID), enquanto as mutações de ganho de função estão relacionadas com linfomas e leucemias. Do mesmo modo, as mutações germinativas da *STAT3* são responsáveis por 2 tipos distintos de doenças humanas. As mutações de perda de função do *STAT3* causam a síndrome de hiper-IgE autossómica dominante, enquanto as mutações de ganho de função do *STAT3* induzem linfoproliferação e poli-autoimunidade, adenomas hepatocelulares inflamatórios e vários tipos de cancro, incluindo linfomas e leucemias. Estudos pré-clínicos indicam que a inibição de *JAK3* com compostos como Nigericina e JANEX-1 pode ter efeitos terapêuticos, induzindo apoptose e reduzindo o crescimento tumoral no CRC. Além disso,

*JAK3* tem sido associado à exaustão das células T no microambiente tumoral, enfraquecendo a resposta imunitária contra o cancro.

O objetivo do presente estudo foi investigar o papel de JAK3 e STAT3 no CRC, tanto em termos epigenéticos quanto genéticos. Para tal, realizou-se uma análise inicial da metilação do gene *STAT3*, utilizando dados públicos do TCGA Wanderer e dados internos. A análise não revelou diferenças significativas na metilação do gene *STAT3* entre tecidos tumorais e normais, exceto em duas sondas CpG no corpo do gene, sem impacto na sua expressão. Com base nesses resultados, a investigação foi ampliada para outros genes da via de sinalização STAT3, com uma abordagem computacional e bibliográfica que identificou 16 genes. A análise de co-expressão usando o cBioPortal e o conjunto de dados TCGA PanCancer CRC (n=524) revelou que 11 genes mostraram correlações positivas significativas com a expressão de STAT3 (q-value < 0,001), enquanto um gene, PIM1, não mostrou associação significativa. Uma análise da expressão diferencial entre os cancros colorretais MSI e MSS (CRC) revelou que 11 dos 17 genes selecionados apresentavam níveis de expressão significativamente alterados nos tumores MSI ($p < 0,01$). Estes genes foram submetidos a uma análise de metilação do promotor realizada através do TCGA Wanderer, que revelou hipermetilação significativa do JAK3 em duas sondas CpG ($p < 0,01$). Esta análise foi replicada em 82 amostras tumorais usando arrays Illumina EPIC, que fornecem uma maior resolução. Nesta análise*, JAK3* apresentou hipermetilação elevada, particularmente em tumores MSI, juntamente com mutações no gene *BRAF*.

A avaliação da metilação do promotor de *JAK3* foi posteriormente expandida para cinco linhas celulares de CRC (DLD-1, HCT116, HT-29, LS174T e SW480) e uma linha celular de cancro do intestino delgado (HuTu-80, utilizada como controlo). Esta avaliação interrogou 36 de 88 locais na ilha CpG em que os níveis de metilação média variaram significativamente entre as linhas celulares de CRC, com a LS174T apresentando a menor metilação (60,99%) e HCT116 a maior (94,75%). A linha HuTu-80 exibiu o nível mais baixo de metilação global (51,79%). Por conseguinte, o *JAK3* está altamente metilado nas linhas celulares de CRC, com mais de metade dos locais interrogados a apresentarem metilação.

Para determinar se a metilação do promotor de JAK3 influenciava a expressão de ARNm nas linhas celulares, estas foram tratadas com Azacitidina (AZA), um agente que inibe as ADN metiltransferases. A nível basal, *JAK3* revelou ter uma baixa expressão de ARNm em todas as linhas exploradas. O tratamento com AZA foi avaliado após 48 e 72 horas de tratamento, uma vez que a desmetilação requer pelo menos uma mitose para ocorrer. No entanto, o tratamento com AZA não apresentou qualquer efeito drástico na expressão do ARNm de JAK3 em nenhuma das linhas celulares, com exceção da HuTu-80 às 48h, mas não às 72h. A falta de uma resposta clara ao tratamento com AZA pode dever-se à falta de ativadores transcricionais essenciais, à presença de repressores transcricionais ou a efeitos mais complexos e indiretos devido a uma resposta pleiotrópica à AZA. Em conjunto, estas experiências não conseguiram demonstrar um efeito claro da metilação de JAK3 e da expressão genética, pelo menos na ilha CpG associada ao promotor estudado.

Apesar da baixa expressão génica de *JAK3*, procurámos investigar se esses níveis baixos eram suficientes para produzir níveis observáveis de proteína de JAK3. Os estudos de expressão proteica foram efetuados não só no JAK3, mas também em STAT3 e STAT3 fosforilado (pSTAT3) nas várias linhas celulares apresentadas anteriormente. Embora JAK3 não ter sido detetado nos extratos proteicos das linhas celulares analisadas, todas as linhas mostraram expressão de STAT3, com HT29 e DLD-1 apresentando os níveis mais elevados. SW480 destacou-se pela elevada fosforilação de STAT3, particularmente na fração insolúvel.

A discrepância entre os padrões de metilação de JAK3 e a expressão proteica sugere que podem estar envolvidos mecanismos reguladores adicionais. Estes podem incluir modificações das histonas, que podem funcionar em conjunto com a metilação do ADN para regular a expressão genética, ou a regulação pós-transcricional por microARNs. Também levanta a possibilidade de mecanismos

compensatórios dentro da via JAK/STAT3. Outros membros da família JAK, como JAK1 ou JAK2, poderiam compensar a perda da função de JAK3, mantendo a sinalização de STAT3. Em especial, JAK1 poderia ter este comportamento, uma vez que pode cooperar com JAK3 na sinalização através de recetores contendo γc. Esta redundância na via poderia explicar por que razão a ativação de STAT3 persiste apesar da hipermetilação de *JAK3* e da falta de expressão da proteína.

Este estudo apresentou algumas limitações, tais como a falta de variabilidade na metilação do promotor *JAK3* entre as linhas celulares de CRC selecionadas, que não representavam com precisão os diversos padrões de metilação observados em amostras primárias de CRC. Esta uniformidade nas linhas celulares, associada à incapacidade de restaurar a transcrição de *JAK3* através da desmetilação, dificultou a investigação do papel do silenciamento de *JAK3* no CCR. Para colmatar estas limitações, a investigação futura poderia beneficiar da inclusão de linhas celulares de CRC conhecidas por expressarem JAK3, tais como CaR-1 ou SW837, ou através do estudo da expressão de JAK3 em amostras de tumores primários com diferentes estados de metilação. Além disso, a expansão do âmbito para analisar outros genes candidatos na via STAT3, como SOCS1, poderia fornecer informações valiosas sobre os complexos mecanismos reguladores em jogo no CRC.

**Palavras-chave:** Cancro colorretal, STAT3, JAK3, metilação do ADN, linhas celulares de cancro

# Table of Contents

# List of Figures



# List of Tables

## List of Abbreviations, Acronyms and Symbols

| | |
|---|---|
| **5-FU** | 5-Fluorouracil |
| **ACOX1** | Acyl-CoA Oxidase 1 |
| **Alu** | Short Interspersed Repetitive Element |
| **APC** | Adenomatous Polyposis Coli |
| **APCs** | Antigen-Presenting Cells |
| **AZA** | 5'-Aza-2'-Deoxycytidine (also known as Decitabine) |
| **B7-1/B7-2** | CTLA-4 |
| **BCL2** | B-Cell Lymphoma 2 |
| **BCL2L1** | B-Cell Lymphoma 2-Like 1 (also known as Bcl-xL) |
| **BRAF** | B-Raf Proto-Oncogene, Serine/Threonine Kinase |
| **Bcl-2** | B-Cell Lymphoma 2 |
| **Bcl-xL** | B-Cell Lymphoma-Extra Large |
| **COAD** | Colon Adenocarcinoma |
| **COX-2** | Cyclooxygenase-2 |
| **CRC** | Colorectal Cancer |
| **cDNA** | Complementary DNA |
| **c-Jun** | Protein Involved in Cell Proliferation |
| **CD4+** | Cluster of Differentiation 4 Positive |
| **CD8+** | Cluster of Differentiation 8 Positive |
| **CDKN1A** | Cyclin Dependent Kinase Inhibitor 1A (also known as p21) |
| **CMS** | Consensus Molecular Subtypes |
| **COBRA** | Combined Bisulfite Restriction Analysis |
| **EDTA** | Ethylenediaminetetraacetic Acid |
| **EGF** | Epidermal Growth Factor |
| **EGFR** | Epidermal Growth Factor Receptor |
| **FAP** | Familial Adenomatous Polyposis |
| **Fas** | Fas Cell Surface Death Receptor |
| **FGF** | Fibroblast Growth Factor |
| **FGFR** | Fibroblast Growth Factor Receptor |
| **FOLFOX** | Combination of 5-Fluorouracil and Oxaliplatin |
| **FOLFIRI** | Combination of 5-Fluorouracil and Irinotecan |
| **G1/S-Phase** | Transition Phase in the Cell Cycle |
| **GAPDH** | Glyceraldehyde-3-Phosphate Dehydrogenase |
| **GFAP** | Glial Fibrillary Acidic Protein |
| **HER2** | Human Epidermal Growth Factor Receptor 2 |
| **IAPs** | Inhibitor of Apoptosis Proteins |
| **ICI** | Immune Checkpoint Inhibitor |
| **IFNs** | Interferons |
| **IFNG** | Interferon Gamma |
| **IgE** | Immunoglobulin E |
| **IL-2Rβ** | Interleukin-2 Receptor Beta |
| **IL-2Rγ** | Interleukin-2 Receptor Gamma |
| **IL-6** | Interleukin 6 |
| **ILs** | Interleukins |
| **JANEX-1** | A JAK3 Inhibitor |
| **JAK/STAT3** | Janus Kinase/Signal Transducer and Activator of Transcription 3 Pathway |
| **KRAS** | Kirsten Rat Sarcoma Viral Oncogene Homolog |
| **LIF** | Leukaemia Inhibitory Factor |

| | |
|---|---|
| **LB** | Lysogeny Broth |
| **LINE-1** | Long Interspersed Nuclear Element-1 |
| **MHC** | Major Histocompatibility Complex |
| **MCL1** | Myeloid Cell Leukaemia 1 |
| **mCRC** | Metastatic Colorectal Cancer |
| **mRNA** | Messenger RNA |
| **MSI** | Microsatellite Instability |
| **MSS** | Microsatellite Stable |
| **PD-1** | Programmed Death-1 |
| **PD-L1** | Programmed Death-Ligand 1 |
| **PD-L2** | Programmed Death-Ligand 2 |
| **PDGFR** | Platelet-derived growth Factor Receptor |
| **PI3K/AKT** | Phosphatidylinositol 3-Kinase/Protein Kinase B Signalling Pathway |
| **POLE** | DNA Polymerase Epsilon Catalytic Subunit |
| **p53** | Tumour Suppressor Protein |
| **pJAK3** | Phosphorylated Janus Kinase 3 |
| **pSTAT3** | Phosphorylated Signal Transducer and Activator of Transcription 3 |
| **RCT-PCR** | Reverse Transcription Polymerase Chain Reaction |
| **READ** | Rectum Adenocarcinoma |
| **RSEM** | RNA-Seq by Expectation Maximization |
| **MAPK** | Mitogen-Activated Protein Kinase Signalling Pathway |
| **SCID** | Severe Combined Immune Deficiency |
| **SCNAs** | Somatic Copy Number Alterations |
| **SH2** | Src Homology 2 Domain |
| **SINE** | Short Interspersed Nuclear Element |
| **Src** | Src Kinase Family |
| **STAT** | Signal Transducer and Activator of Transcription |
| **SOC** | Super Optimal Broth with Catabolite Repression |
| **SOCS1** | Suppressor of Cytokine Signalling 1 |
| **TBE** | Tris-Borate-EDTA (buffer solution) |
| **TE** | Tris-EDTA (buffer solution) |
| **TGF-β** | Transforming Growth Factor Beta |
| **TIL** | Tumour-Infiltrating Lymphocytes |
| **TMB** | Tumour Mutation Burden |
| **TME** | Tumour Microenvironment |
| **TPT-1** | Translationally Controlled Tumour Protein |
| **VEGF** | Vascular Endothelial Growth Factor |
| **VEGFR** | Vascular Endothelial Growth Factor Receptor |
| **Y705** | Tyrosine Residue at Position 705 |
| **γc** | Common Cytokine Receptor Gamma Chain |
| * | $p < 0.05$ |
| ** | $p < 0.01$ |
| *** | $p < 0.001$ |

# I. Introduction

## 1.1. Colorectal cancer

### 1.1.1. Incidence, molecular characterization and taxonomy

Colorectal cancer (CRC) is the third most common cancer in the world and the second highest in mortality, having a very high incidence in the Iberian Peninsula, where it remains the most diagnosed type of cancer. (**Figure 1.1**). The incidence of CRC is also increasing in various developing countries.[1] CRC arises from the accumulation of multiple genetic and epigenetic alterations affecting genes involved in cell replication, genome maintenance and apoptosis, that transform normal epithelial cells into invasive adenocarcinomas.

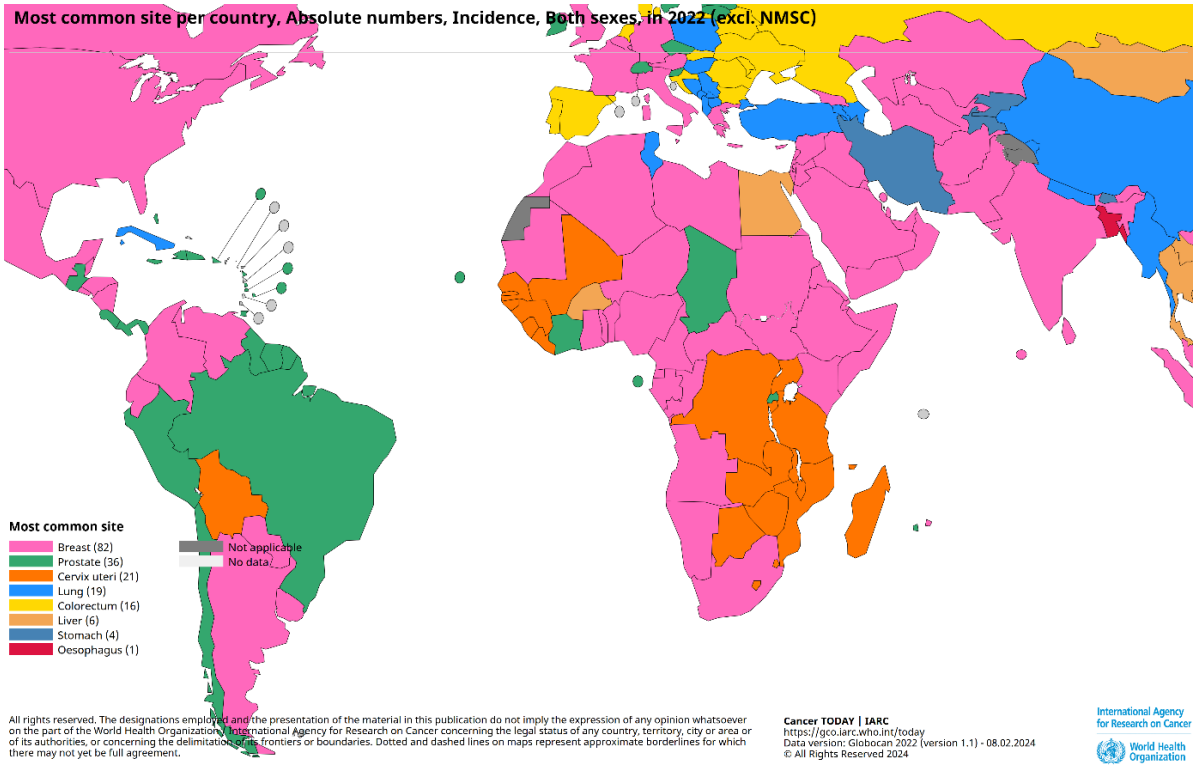


**Figure 1.1- Incidence of most common cancer per country.** Reproduced from Cancer TODAY | IARC

The most frequent mutation in CRC is the inactivation of adenomatous polyposis coli gene (*APC*). APC binds to β-catenin, suppressing the proliferative Wnt-signalling pathway. Other relevant mutations affect tumour suppressor genes, such as *TP53,* and proto-oncogenes like *KRAS* and *BRAF.* In addition to genetic mutations, epigenetic alterations, including post-translational modifications of histones, non-coding RNAs, and DNA methylation, play a significant role in CRC. Histone modifications, such as acetylation, methylation, ubiquitination, phosphorylation, and SUMOylation, regulate chromatin structure and gene expression.[2] Non-coding RNAs can result in the degradation of the target mRNA or inhibition of its translation into protein. DNA methylation, particularly when it occurs in promoter regions and Cytosine-Guanine-rich (CG) sequences termed CpG islands, generally acts to repress gene transcription.[3] All these epigenetic mechanisms play a crucial role in establishing and maintaining transcriptional programs specific to each cell lineage in healthy tissues but are often altered in cancer cells, contributing to the transcriptional dysregulation that drives malignant transformation.

Aberrant DNA methylation is one of the hallmarks of cancer, and likely the most studied and best understood epigenetic alteration in cancer. In humans, DNA methylation occurs almost exclusively at cytosine residues in CpG dinucleotides. The majority of CpG dinucleotides in the human genome are methylated, but there are CpG-rich 200-2000 bp long sequences called CpG islands, which are typically unmethylated in normal healthy cells. These sequences are frequently found in the promoter regions of approximately 40-60% of human genes, where they regulate of gene expression.[3] Methylated CpG dinucleotides are usually found in gene bodies and large repetitive sequences, such as long interspersed nuclear element (LINE-1), short interspersed nuclear element (SINE)/Alu sequences, and other retrotransposon elements. In general, the normal methylation pattern is profoundly altered in cancer cells.[2] In CRC, nearly all tumours display multiple alterations in their DNA methylation profile.

CRC is classified into three categories based on genetic and familial components: sporadic, familial, and hereditary. Sporadic CRC is the most common form, accounting for approximately 70% of all CRC cases. It occurs in individuals without a family history or known genetic predisposition to CRC. Most cases are diagnosed in people aged 50 or older. Familial CRC accounts for about 25% of cases. It occurs in families with multiple members affected by CRC but without a specific hereditary syndrome identified. The risk increases if a first-degree relative has CRC, especially if diagnosed before age 50. Hereditary CRC is less common, comprising about 5% of cases.[4] It is associated with specific inherited genetic mutations with high penetrance. These hereditary syndromes include Lynch Syndrome (Hereditary Non-Polyposis Colorectal Cancer), Familial Adenomatous Polyposis (FAP), and others.[5]

CRC is very heterogeneous in terms of its molecular characteristics, with two very distinct types based on the number of mutations: Hypermutated tumours represent around 15% of the sporadic cases, and are characterised by a high mutation burden but low chromosomal instability, typically including tumours with microsatellite instability (MSI) or DNA polymerase epsilon catalytic subunit (*POLE*) mutations; Non-hypermutated tumours, encompassing most sporadic CRC cases, show a lower number of mutations but exhibit strong chromosomal instability. In 2015, a molecular classification based on the transcriptomic profiles of 6 different CRC cohorts proposed four consensus molecular subtypes (CMSs 1-4) (**Figure 1.2**), correlating with disease progression and clinical outcomes: [6]

- CMS1 (microsatellite instability immune, 14%) enclosed most MSI tumours. These were also found to be hypermutated, with a low incidence of somatic copy number alterations (SCNAs), and a high incidence of *BRAF* V600E mutation. Another feature was the extensive hypermethylation and CpG Island Methylator Phenotype (CIMP)-high status, which is characterized by the extensive methylation of the promoters of several genes[7].
- CMS2 (canonical, 37%) tumours are characterized by epithelial differentiation and strong upregulation of Wnt and MYC downstream targets, both implicated in CRC carcinogenesis. Along with this, there was a more frequent gain of somatic copy number alterations (SCNA-high) in oncogenes and losses in tumour suppressor genes compared to other subtypes.
- CMS3 (metabolic, 13%) although characterized as chromosomal instability, it showed some distinct patterns, with fewer hypermutated SCNAs which overlapped with MSI status, and there were overall intermediate levels of gene hypermethylation, consistent with a CIMP-low status. Another important trait is the overrepresentation of *KRAS* mutations, that in turn arise the prominent metabolic adaptation and consequently the multiple metabolism signatures present in the CMS3 epithelial CRCs.
- CMS4 (mesenchymal, 23%) tumours have high SCNAs and low level of mutations. They show upregulation of genes implicated in epithelial-mesenchymal transition (EMT), along with transcriptional signatures associated with the activation of transforming growth factor β (TGF-β) signalling, angiogenesis, matrix remodelling pathways and complement inflammatory system. These tumours displayed worse survival and relapse-free survival, as they also tend to be diagnosed at more advanced stages.

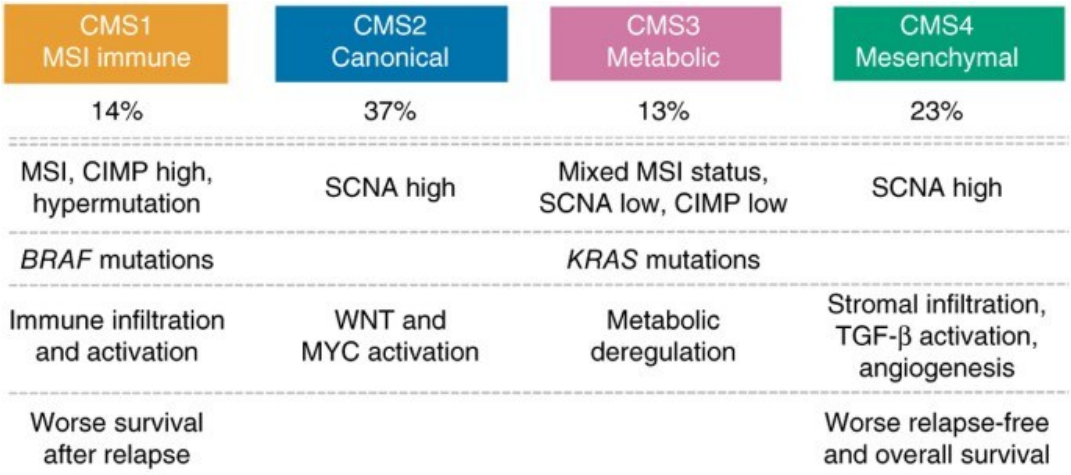


**Figure 1.2-Taxonomy of CRC.** Biological differences in genetics and epigenetics, immune response, angiogenesis, metabolism and prognosis of the 4 current subtypes of CRC, as proposed by Guinney et al. [6]

### 1.1.2. Therapeutic Approaches in CRC

Advances in primary and adjuvant treatments have steadily improved survival for patients with CRC. The standard CRC treatment is surgical resection of the primary tumour and, if possible, local metastases. Surgical resection is often followed by chemotherapy depending on the tumour stage and its MSI status. However, for patients with unresectable lesions or who cannot tolerate surgery, the goal is to achieve the maximum shrinkage of the tumour and suppress further tumour spread and growth. Radiotherapy and chemotherapy are the leading strategies for controlling disease in such patients. Chemotherapy has become the backbone of CRC treatment, especially for metastatic cases, extending overall survival to nearly 20 months. Fluoropyrimidines, mainly 5-fluorouracil (5-FU), have been especially effective, with a response rate of 20%. Combined therapies of 5-FU with oxaliplatin (FOLFOX) and irinotecan (FOLFIRI) have significantly improved the response rate and overall survival of CRC patients.[8] Despite the advancements in detection and treatment, CRC continues to be a very important challenge in healthcare. The urgent need for innovative therapies persists, especially for individuals facing metastatic CRC. Developing novel and effective treatment approaches remains a critical priority in oncology research and clinical practice.

Targeted therapies have improved CRC treatment, directly inhibiting cancer cell proliferation, differentiation, and migration. These therapies target specific vulnerabilities of cancer cells while limiting their effect in normal cells. Especially relevant agents are monoclonal antibodies targeting the epidermal growth factor receptor (EGFR) pathway (e.g. cetuximab and panitumumab)[8,9] or the vascular endothelial growth factor (VEGF) pathway (e.g. bevacizumab)[10]. Binding of EGF to its receptor triggers various downstream intracellular signalling pathways such as the MAPK, PI3K/AKT, and JAK/STAT3. These pathways regulate cell growth, survival, and migration. The VEGF/VEGFR pathway is critical for angiogenesis —the formation of new blood vessels— and plays a vital role in tumour initiation, growth, and metastasis. Angiogenesis is additionally regulated by other extracellular factors beyond VEGF, including fibroblast growth factors, TGFs, platelet-derived endothelial cell growth factors, and angiopoietins produced by cancer or stromal cells.[11]

More recently, immunotherapies have achieved unprecedented long-term responses in tumours that were previously challenging to treat such as melanoma and lung cancer. These therapies enhance the immune system's recognition and response against cancer cells, which often evade immune detection by secreting immunosuppressive factors, e.g. TGF-β and Interleukin-6 (IL-6), recruiting regulatory cells

or downregulating major histocompatibility complex 1. Several strategies to enhance the immune response against cancer cells have been developed.[12] Immune checkpoint inhibitors (ICIs) are a class of cancer immunotherapies that have revolutionized the treatment of various malignancies. These therapies work by targeting specific proteins involved in immune system regulation, particularly those that act as "checkpoints" to prevent excessive immune responses. By blocking these checkpoint proteins, ICIs effectively release the brakes on the immune system, allowing it to recognize and attack cancer cells more effectively. The most well-known and widely used ICIs target proteins such as CTLA-4 (cytotoxic T-lymphocyte-associated protein 4), PD-1 (programmed cell death protein 1), and PD-L1 (programmed death-ligand 1). CTLA-4 and PD-1 inhibitors were the first immune checkpoint inhibitor therapy approved for CRC.

The efficacy of ICIs relies on the recognition of the malignant cells by the immune system, i.e. the pre-existing inflammatory microenvironment characterized by a high level of tumour-infiltrating lymphocytes (TIL), that exposes the tumour cells to cytotoxic destruction. These highly infiltrated tumours are known as “hot” tumours.[13] There is a clear association between the number of mutations and immunogenicity. In general, tumours with a high number of mutations, i.e. high tumour mutation burden (TMB), elicit a stronger immune response and are, in principle, more susceptible to ICI treatments. On the other hand, tumours with low lymphocyte infiltration, known as “cold” tumours, exhibit poor response to ICIs. In line with this, the hypermutated MSI CRCs exhibit higher immune infiltration (**Figure 1.2**). However, MSI tumours represent only 15% of primary CRCs, and their prevalence drops to 3-5% of the metastatic CRCs (mCRC).[14–16] Currently, ICIs are only approved for treatment of MSI mCRC, where they have achieved a moderate response rate, generally below 50%. MSS mCRCs are excluded from ICI treatment, since the objective response is generally below 10%. Notably, TMB is not the only factor modulating lymphocyte infiltration (**Figure 1.3**). In fact, around 30% of the MSI tumours exhibit low lymphocyte infiltration despite their high TMB. Conversely, over 25% of the MSS CRCs exhibit very high lymphocytic infiltration despite having a lower TMB.[17]

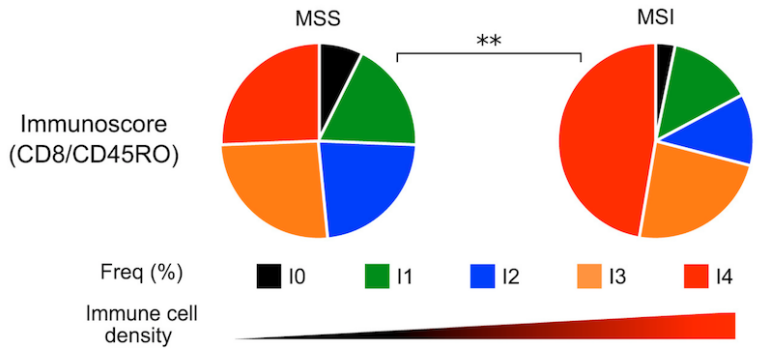


**Figure 1.3- Immunoscore in MSS and MSI.** The frequency of Immunoscore-based groups (I0, I1, I2, I3, I4) in MSS and MSI patients. Immunoscore summarizes the density of memory (CD45RO) and cytotoxic (CD8) T cells in the CT and in the IM of the tumour. Adapted from Mlecnik et al.[17]

Therefore, MSS tumours exhibiting high immune infiltration could potentially respond to ICIs regardless of their TMB. However, the molecular factors driving immune infiltration in MSS CRCs are not well understood. Most likely, tumour immunogenicity responds to a complex multifactorial network of interactions between cancer cells, stroma cells, and immune cells. Identifying these factors can provide novel therapeutic approaches to enhance tumour immunogenicity and, consequently, improve the therapeutical response to ICIs. Ultimately, these advancements aim to improve patient outcomes and increase survival rates.

## 1.2. Janus Kinase (JAK) and Signal transducer and activator of transcription (STAT) pathways

### 1.2.1. General view of the JAK/STAT pathway

The Janus kinase-signal transducer and activator of transcription (JAK-STAT) pathway is a fundamental signalling mechanism that transmits signals from extracellular cytokines, growth factors, and other ligands to the nucleus, thereby regulating gene expression and orchestrating diverse cellular functions. This pathway plays an essential role in immune responses, cell growth, differentiation, survival, and homeostasis, making it a key player in both normal physiology and disease pathology (**Figure 1.4**).[18] The JAK protein family consists of four members in mammals: JAK1, JAK2, JAK3 and the alternatively named tyrosine kinase 2 (TYK2). STAT proteins are a family of latent cytoplasmic transcription factors comprising seven members: STAT1, STAT2, STAT3, STAT4, STAT5a, STAT5b, and STAT6.[19] The JAK-STAT signalling process begins with the binding of cytokines, including interferons (IFNs), ILs [18] or growth factors to their corresponding receptors, which are constitutively associated with JAKs. Upon ligand-receptor interaction, JAKs undergo auto- or transphosphorylation, leading to the phosphorylation of specific tyrosine residues on the receptor tails. These phosphorylated residues create docking sites for latent STAT proteins, which bind to the receptor complex through their SH2 domains and are themselves phosphorylated by JAKs. Once phosphorylated, STATs dissociate from the receptor, dimerize (forming either homodimers or heterodimers), and translocate to the nucleus, where they bind to target gene promoters to regulate transcription.[20,21]

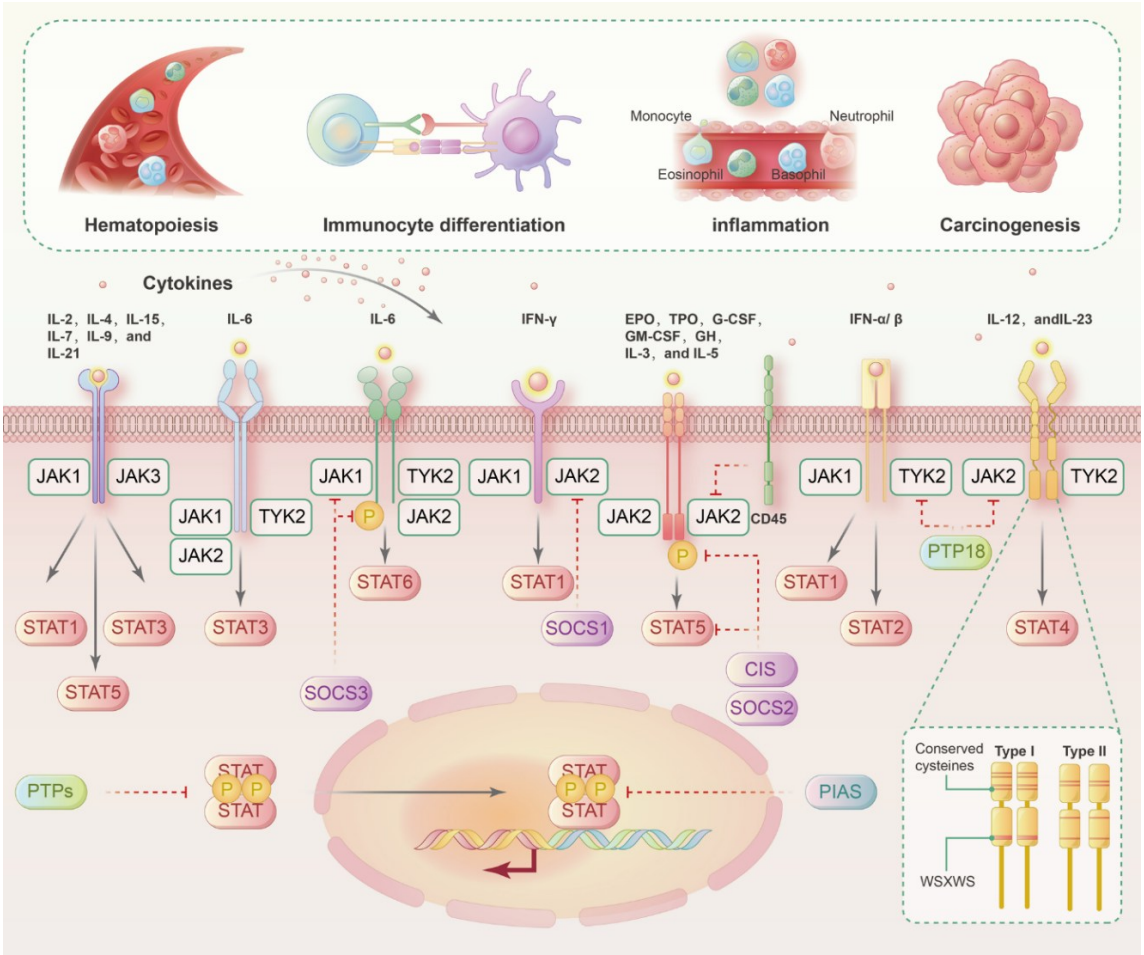


**Figure 1.4- JAK-STAT pathways.** This figure illustrates both the canonical activation and negative regulation of the JAK-STAT signalling pathways. In canonical activation, cytokines bind to their receptors, causing a conformational change that recruits and activates JAKs through phosphorylation. This leads to the phosphorylation

of receptor tyrosines, creating docking sites for STATs. The phosphorylated STATs then dissociate from the receptor, form dimers, enter the nucleus, and regulate gene transcription. Obtained from Xue, C. et al.[18]

### 1.2.2. JAK3 and STAT3

The human *Janus Kinase 3* gene (*JAK3*), located at 19p13.11, exhibits the most restricted expression pattern among the four *JAK* genes. It is mainly expressed in hematopoietic cells belonging to the lymphoid compartment and certain myeloid cell subpopulations[22], as well as in endothelial and mitotic cells in both hematopoietic and non-hematopoietic organs.[23] Loss-of-function mutations in JAK3 are associated with 5% of the cases of severe combined immune deficiency (SCID), while gain-of-function mutations are related to lymphomas and leukaemias.[22] Similarly, germline mutations of STAT3 are responsible for 2 distinct types of human diseases. STAT3 loss-of-function mutations cause autosomal-dominant hyper-IgE syndrome, while STAT3 gain-of-function mutations induce lymphoproliferation and poly-autoimmunity, inflammatory hepatocellular adenomas and several types of cancer, including lymphomas and leukaemia's. [24] [25,26]

JAK3 activation is triggered by cytokine binding to the IL-2 receptor subunit gamma or IL-2Rγ. Cytokines that activate the common cytokine receptor γ chain (γc) family include IL-2, IL-7, IL-9, IL-21, IL-4, and IL-15, the two latter being implicated in CRC pathogenesis [27]. Most of these cytokines can also activate STAT3.[18,28]Activated IL2Rβ recruits JAK1 and JAK3 to the cell membrane through its intracellular domain and triggers their phosphorylation. In the canonical pathway (**Figure 1.4),** activated JAK1 and JAK3 phosphorylate STAT5A in a specific tyrosine residue, inducing the translocation of this transcription factor into the nucleus[29]. Nonetheless, JAK3 is also able to activate STAT1, STAT5B[21,30] and STAT3.[27,31,32] For example, the cytokine IL-15 increases phosphorylated JAK3 and STAT3 (pJAK3 and pSTAT3, respectively) levels in skeletal muscle cells, which in turn leads to the promotion of Glucose transporter 4 translocation and consequently glucose uptake. In contrast, there was no increase in the phosphorylation or total protein levels of JAK1 and STAT5 in cells treated with IL-15[31]. STAT3 is activated by various extracellular factors, including interleukins (e.g., IL-6, IL-11), Oncostatin M, and leukaemia inhibitory factor (LIF).[33,34]Other molecules like epidermal growth factor (EGF), fibroblast growth factor (FGF), TGF-β, and retinoic acid can also activate STAT3 signalling. Upon binding to their membrane receptors (e.g., EGFR, PDGFR, FGFR),[35–38] these stimuli trigger a cascade leading to the phosphorylation of STAT3 at tyrosine residue Y705, which is essential for its dimerization and subsequent DNA binding[39]. Cytoplasmic kinases such as the Src kinase family and pyruvate kinase can also activate STAT3. While the canonical pathway involves Y705 phosphorylation, STAT3 can also function non-canonically. For example, unphosphorylated STAT3 can still dimerize, translocate to the nucleus, and regulate the expression of genes involved in cell cycle progression and oncogenesis, such as *Cyclin B1* and *E2F*.[40–42]

### 1.2.3. JAK3 in cancer

Constitutive JAK3 activation has been identified in several types of cancers, particularly in human immune cell cancers[27,43]. This is largely due to gain-of-function mutations in *JAK3* across a range of T-cell malignancies. [22] However, alterations have also been found in cancers affecting other hematopoietic cell lineages[44]. *JAK3* has been found altered in solid tumours, due to both somatic gain-of-function mutations as well as loss-of-function mutations. Specifically, *JAK3* alterations have been identified in lung cancer[45], high-grade serous ovarian cancer[46] and glioblastoma[47]. *JAK3* has been associated with T-cell exhaustion in the tumour microenvironment, which very likely occurs due to chronic T-cell receptor stimulation and continuous IL-2 receptor-induced STAT5 phosphorylation in CD4+ and CD8+ T cells.[48] Preclinical studies using the *JAK3* inhibitor PF-06651600 have shown potential in enhancing T-cell responses and reducing tumour load in solid *in vivo* murine tumour models. Additionally, JAK3 inhibition has demonstrated improved antitumor effects, particularly when combined with other

immunotherapies such as anti-PD-1 immune checkpoint inhibitors.[48] In CRC, *JAK3* is rarely mutated (< 3%), according to the information in the cBio cancer genomics portal[49]. Inhibition of JAK3 by Nigericin, an antibiotic derived from *Streptomyces hygroscopicus*, promotes apoptosis and autophagy in CRC cell lines such as HCT-116.[50] The *JAK3* inhibitor JANEX-1 (4-(4'-hydroxyphenyl) amino-6,7-dimethoxyquinazoline) prevented intestinal tumorigenesis and markedly improved survival in a multiple intestinal neoplasia (Min) mouse model of Familial Adenomatous Polyposis (FAP, one of the CRC hereditary syndromes), resulting from a single point mutation in the murine homolog of the APC gene. [51] JANEX-1 prevented intestinal tumorigenesis in Min mice and markedly improved survival.[51] Furthermore, a study utilising human cancer cDNA microarrays to identify differentially expressed cancer-related genes in CRC revealed that JAK3 was one of the most highly upregulated genes. The detection of JAK3 mRNA expression in CRC tissue was confirmed through cDNA microarrays and RT-PCR.[52]

### 1.2.4. STAT3 in cancer

STAT3 is frequently dysregulated in cancer and plays a crucial role in tumour development and progression. Constitutive activation of STAT3 is observed in approximately 70% of solid tumours, underscoring its significance in oncogenesis.[53] This aberrant activation often arises from the overactivity of other factors that are upstream in the pathways, such as EGFR, HER2, Src, and JAK2. The consequences of persistent STAT3 activation in cancer lead to more aggressive tumour phenotypes, characterized by enhanced growth and survival, promotion of epithelial-mesenchymal transition (EMT), and increased migration, invasion and therapeutic resistance.[19] Its effects are evident not only within tumour cells but also in the tumour microenvironment. Given its ubiquitous presence and diverse roles in cancer biology, STAT3 has emerged as a prime target for therapeutic interventions in oncology (**Figure 1.5**). [39]

STAT3 promotes tumour cell growth through various mechanisms. It directly upregulates anti-apoptotic genes such as *Bcl-2*, *Bcl-xL*, and *Survivin*, while repressing pro-apoptotic genes like *Fas*, through cooperation between *STAT3* and *c-Jun*. It also enhances cell proliferation by upregulating cyclin D1, which facilitates the G1/S-phase transition[39].

In tumour immune evasion, STAT3 upregulates immunosuppressive cytokines such as IL-10, IL-23 (which reduces CD8+ T cell infiltration and promotes angiogenesis), and TGF-β. Additionally, in complex with EGFR, STAT3 increases Cyclooxygenase-2 (COX-2), which is involved in inflammation and is upregulated in various cancers. [54] STAT3 also undermines tumour suppression by inhibiting p53, a critical defence against malignancy. While p53 mutations are common in colorectal carcinomas, early-stage tumours (adenomas) often show reduced p53 expression. STAT3 inhibits p53 transcription by binding to its promoter. Blocking STAT3 in cancer cells increases p53 expression, leading to apoptosis.[39]

In the tumour microenvironment (TME), STAT3 activation is considered an oncogenic event, with high phospho-STAT3 levels correlating with poor prognosis in various cancer types, including non-small cell lung cancer, gastric cancer, and CRC.[39] STAT3 induces and maintains a pro-carcinogenic inflammatory microenvironment while modulating the host's immune response against tumour cells. It upregulates genes involved in the growth and survival of cancer cells, including cyclins, *Cdc25A, c-Myc,* and IAPs (Inhibitor of apoptosis proteins).[39] STAT3-mediated induction of immunosuppressive factors in the TME, such as IL-6, IL-10, TGF-β, and VEGF, further amplifies STAT3 activation in both tumour cells and tumour-infiltrating immune cells. This activation in cancer cells leads to the release of factors that inhibit the maturation and activation of antigen-presenting cells (APCs), impeding the generation of antigen-specific T cells and promoting immune tolerance.

There are conflicting findings regarding the function of STAT3 in CRC. Certain studies have suggested that high STAT3 expression is a favourable prognostic determinant and inhibits tumour

invasion,[48] while others have reported that high phospho-STAT3 levels are associated with higher mortality and tumour invasion.[55] The inhibition of the JAK3/STAT3 signalling pathway induces apoptosis and cell cycle arrest in colon carcinoma cells (SW480, HT-29) and primary tumours.[56] Although the STAT3 pathway has been a target of interest in CRC, its methylation pattern and the significance of JAK3 have not been thoroughly investigated. STAT3 has been mainly studied in the IL-6/JAK/STAT3 axis, where *JAK1* and *JAK2* are the canonical upstream effectors. Therefore, it is important to understand the specific effects of STAT3 in different tumour types to avoid promoting cancer invasion.[57]

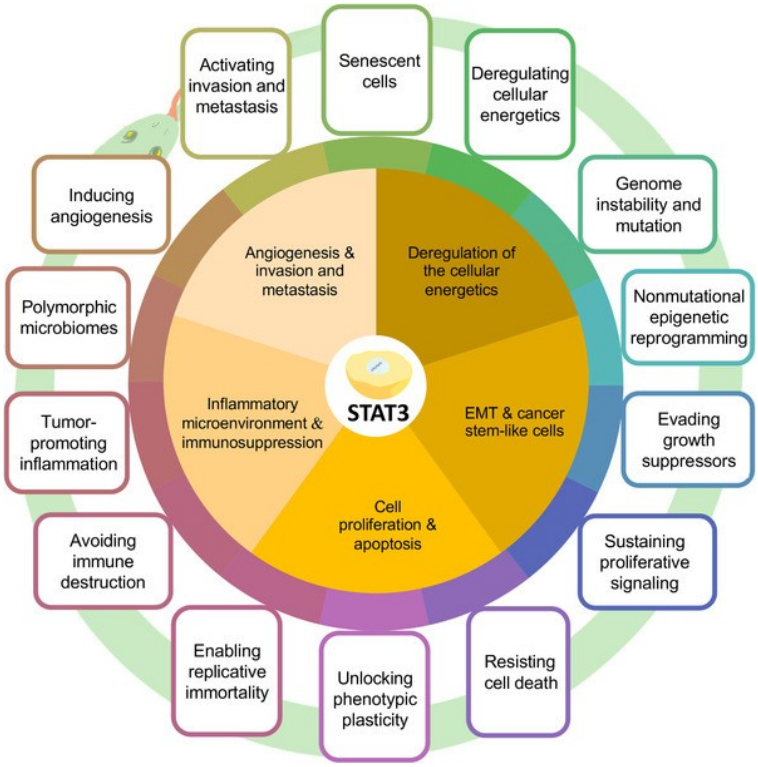


**Figure 1.5 - STAT3 and cancer hallmarks.** STAT3 alterations enhance the manifestation of tumour hallmarks: inflammatory microenvironment and immunosuppression; cell proliferation and apoptosis; epithelial-mesenchymal transition (EMT) and cancer stem-like cells; deregulation of cellular energetics; and angiogenesis, invasion, and metastasis. Adapted from Wang et al. (2022) [19]

# II. Aims

This thesis sought to identify epigenetic and genetic alterations in the JAK3/STAT3 pathway in CRC. To achieve this goal, the following specific objectives were established:

1. To identify genetic and epigenetic alterations in the JAK/STAT3 pathway in human CRC samples
2. To study the relationship between promoter methylation and transcriptional expression of target genes in human CRC cell lines
3. To study the expression patterns of selected members of the JAK/STAT3 pathway in a panel of human CRC cell lines

# III. Materials and methods:

## 3.1. Computational selection of candidate genes

The identification of genes of the STAT3 pathway was conducted through an exhaustive search encompassing several resources. Specifically, the Kyoto Encyclopedia of Genes and Genomes (KEGG) database (KEGG T01001: 6774 (genome.jp)), GeneGlobe platform (STAT3 Pathway | GeneGlobe (qiagen.com)), and relevant literature were consulted to identify both upstream and downstream genes of STAT3 pathway potentially involved in cancer.[19,39,54] The search resulted in 17 genes selected for further analyses (*IL2, IL6, IL10, IFNG, JAK1, JAK2, JAK3, CDKN1A, BCL2, MCL1, BCL2L1, PIM1, MYC, ACOX1, GFAP, SOCS1, STAT3*). To determine their relevance to STAT3 in CRC, an analysis was performed using cBio cancer genomics portal [49,58,59] with the Colorectal Adenocarcinoma (TCGA, PanCancer Atlas) dataset with 524 samples/patients. The list of selected genes was submitted to a co-expression analysis done with RSEM (Batch normalized from Illumina HiSeq_RNASeqV2) in reference to *STAT3*.

## 3.2. Methylation status of genes from STAT3 pathways

TCGA Wanderer: [60] was used to analyse the methylation of selected genes. TCGA Wanderer is an interactive viewer of the methylation profiles from TCGA samples analysed with Illumina 450K Methylation Arrays, displaying the methylation differences between normal and tumour tissues. Colon adenocarcinoma (COAD, n=302) and rectum adenocarcinoma (READ, n=98) datasets were selected. In addition. we also analysed differences in methylation of the selected genes on 82 CRCs profiled at the laboratory using Infinium Methylation EPIC arrays, a platform that interrogates the methylation status of around 850.000 CpG sites throughout the human genome. These tumours were previously characterized for their MSI status, mutations in *BRAF*, *KRAS* and *TP53,* and the level of lymphocyte infiltration (TIL). Clinicopathological information was also available (i.e. age, gender, tumour location).

## 3.3. Methylation status of JAK3 in CRC cell lines

### 3.3.1. Bisulfite primer design

The sequence of the promoter region of JAK3 was downloaded from the Ensembl genome browser (ENSG00000105639), including the location of the transcriptional start site, the identified promoter-associated CpG islands and the corresponding Illumina methylation array probes provided by the in-house data. Each sequence was converted in silico simulating the bisulfite conversion: cytosines in CpG sites were converted to a Y (representing C or T). The remaining cytosines were converted to T. The in silico-transformed sequences were used to design primers amplifying the CpG sites of interest, i.e. those exhibiting significant differences between normal and tumour tissues (TCGA data), and among tumours (in-house data). Primer design was done with Primer3 software 61. Primer sequences are shown in Table 1. Primers were ordered from Invitrogen, Thermo Fisher Scientific. All primers were resuspended in a 0.1X TE buffer (1mM Tris-HCl, 0.1mM EDTA•Na2) at a final concentration of 100µM, verified by measuring the absorbance at 260 nm using a NanoDrop ND-1000 Spectrophotometer (Thermo Fisher Scientific).

**Table 1- Primers for the methylation analysis of *JAK3*.** In lowercase, the bases that become transformed after bisulfite treatment.

| Primers | Amplicon | Sequence |
|---|---|---|
| PB-456-forward | 417 bp | 5'-AGTGGtTtAGGAAAttAAGGGGt-3' |
| PB-457-reverse | | 5'-CCCAATCCCTCCTTCCCAAT-3' |
| PB-458-forward | 265 bp | 5'-TGGGTAAAtTGAGGtAATAAGGG-3' |
| PB-459-reverse | | 5'-aCCCCTTaaTTTCCTaAaCCACT-3' |
| PB-466-forward | 233 bp | 5'-CCTaaCAaCACCCTaCCCCA-3' |
| PB-467-reverse | | 5'-TGGGGtAGGGTGtTGttAGG-3' |

### 3.3.2. Bisulfite conversion of DNA

Genomic DNA (gDNA) from CRC cell lines HCT116 (CCL-247™), DLD1 (CCL-221™), LST174T (CL-188™), SW480 (CCL-228™) and small intestine cancer cell line Hutu-80 (HTB-40™) was previously purified by other researchers in the lab, using a Maxwell 16 Instrument and Maxwell 16 DNA Purification Kit (Cat.#AS1020, Promega) following the manufacturer's instructions. These cell lines were obtained from the American Type Culture Collection (ATCC). Cell lines were maintained under the recommended culture conditions suggested by the ATCC. Genomic DNA was subjected to bisulfite conversion using the EZ DNA Methylation™ Kit (Cat. #D5002, Zymo Research), following the manufacturer´s instructions. The bisulfite-treated DNA samples were stored at -20°C until further use.

Bisulfite treatment converts unmethylated cytosines into uracils, while methylated cytosines remain unchanged. These uracils are substituted by thymines by the Taq polymerase during the DNA replication process. Thus, originally methylated cytosines appear as cytosines whereas originally unmethylated cytosines appear as thymines in the final PCR amplicon.

All sets of primers were tested using the HotStarTaq polymerase kit from Qiagen (cat#203205) with a 1ng/µl mix of bisulfite-treated genomic DNA from five cell lines (DLD-1, LS174T, HCT116, HT29 and SW480), 1X PCR buffer, 0.125 µM dNTP, 0.4 µM primers, 0.5X Q-solution and 0.05 units/µl HotStarTaq DNA Polymerase. To determine optimal annealing temperature of every reaction, we performed gradient PCRs (Tm=[50-60°C]), resolving the products by agarose gel electrophoresis. The optimal annealing temperatures for PCR-A (PB-458 and PB-466) and PCR-B (PB-467 and PB-457) were 55°C and 59°C, respectively. For gel electrophoresis, each sample was loaded with Orange G 1x and run in VWR Mini Electrophoresis System (COSMO BIO, LTD) with TBE 1x. Due to technical difficulties, for PCR-B it was used Taq Polymerase- POL II Supreme from NZYTECH, cat#MB35502 (**Table 2**), but keeping the same annealing temperature. These sets of primers were then used to amplify the genomic DNA from each cell line and then checked with Sanger sequencing (StabVida, Lisbon) to confirm they had the sequence needed.

**Table 2- PCR amplifications conditions.**

| Enzyme | Denaturation | Denaturation | Annealing | Extension | Nr. of cycles |
|---|---|---|---|---|---|
| HotStart Quiagen | 95˚C – 15min | 95˚C – 30s | 55˚C; 59 ˚C– 30s | 72˚C – 30s-5min | 35 |
| Taq Flexi Promega | 95˚C – 10min | 95˚C – 15s | 58˚C – 30s | 72˚C –1min-5min | 30 |
| Pol Supreme Nzytech | 94˚C – 5min | 95˚C – 30s | 59˚C – 30s | 72˚C – 30s-5min | 35 |

### 3.3.3. PCR cloning protocol

To clone PCR products, we employed the StrataCloneTM PCR Cloning Kit (Cat. #240205, Agilent Technologies) using the provided protocol with the following adaptations: the ligation reaction was always performed with 1.5 µL of StrataClone Cloning Buffer; 1 µL of the PCR product and another with the control insert; and 0.4 µL of StrataClone Vector Mix amp/kan. This ligation was then incubated for 5 min at room temperature and then placed on ice. Twenty µL of the StrataClone Solo Pack of competent cells expressing the Cre recombinase were mixed with 1 µL of the ligation reactions and incubated for 20 minutes on ice. The transformation mixture was then heat-shocked at 42°C for 45 seconds and incubated again on ice for 10 minutes. Two hundred µL of pre-warmed (at 37°C) of SOC medium were added to the mixture, and then placed at 37°C in agitation for 1h. Meanwhile, LB plates with ampicillin (100 µg/mL) were prepared for blue-white colony screening by spreading 40 µL of 2% w/v X-gal on each plate. One hundred µL of the transformation mixture were seeded on these plates and incubated overnight at 37°C.

### 3.3.4. Colony PCR and Sanger sequencing

Cloning was verified by colony PCR. Briefly, white bacterial colonies were picked from the antibiotic-supplemented culture plates with a pipette tip and directly placed in PCR tubes containing the reaction mixture for GoTaq® Flexi DNA Polymerase (Promega, Cat. #M7806)). Colony PCR details are in **Table 2.** Universal primers T3-F(5'AATTAACCCTCACTAAAGGGAA3') and T7-R (5'GTAATACGACTCACT ATAGG3') were used. PCR products were verified by gel electrophoresis. Then, to remove any unconsumed dNTPs and primers, PCR products were treated with ExoSAP-IT™ (78201.1.ML, Thermo). One µL of ExoSAP was added per 4 µL of PCR product (1:5 dilution) and the mixture was incubated in the Thermocycler for 30 minutes at 37°C and 15 minutes at 80°C. After this treatment, PCR amplicons were prepared for sequencing with the following components: 250 ng of Exosap cleaned PCR and 3 µL 10 µM T3 primer into a final volume of 13 µL. Samples were sent to an external sequencing service (Stabvida), that provided the sequences in abi format (electropherograms). To analyse the sequences, the Benchling platform [62] was used. The sequences were aligned with the *in silico* converted DNA used as the template, where all CpG sites were substituted by YpG. For each CpG site, the methylation status was determined as follows: sites that appeared as TpG were marked as unmethylated, and sites that appeared as CpG were marked as methylated. We employed an in-house R-script to generate visual representation of methylated or unmethylated sites, along with their location, average methylation per CpG site, correlation, and perform statistical analysis using one-way ANOVA and post-hoc Tukey HSD test, with p-value < 0,05 being statistically significant.

## 3.4. JAK3 expression studies

### 3.4.1. Design of primers

The primers to quantify *JAK3* mRNA expression were designed on its cDNA FASTA sequence, obtained from NCBI [63], using the online tool Primer3 (Primer3 Input), with Tm values ranging from 57 to 60 ºC. To favour the amplification of the mature mRNA, primer pairs were designed on consecutive exons present in all the alternative splicing mRNA forms described in the NCBI and as close to the 3' end as possible to exclude short non-functional mRNAs. The primers were ordered from Thermo Scientific (USA) and are shown in Table 3. The lyophilized primers were resuspended in 0.1X TE, the concentration was determined by spectrophotometry at 260nm/280nm using a Nanodrop apparatus. Finally, working aliquots at 10µM were prepared and stored at -20ºC for their future use.

**Table 3– Primers for mRNA expression**

| Primer | Sequence |
|---|---|
| PB-462-Forward (exon21-22) | 5'TCTTCTCTCGCCAGTCAGAC3' |
| PB-463-Reverse (exon 21-22) | 5'CCTCCTCCAGCAGTTCCAA3' |
| PB-464-Forward (exon 22-23) | 5'CTCTTGGAACTGCTGGAGGA3' |
| PB-465-Reverse (exon 22-23) | 5'AGCAGTGAAGGCATGAGTCT3' |
| GAPDH-Forward | 5'GAAGGTGAAGGTCGGAGT3' |
| GAPDH-Reverse | 5'GAAGATGGTGATGGGATTTC3' |
| TPT1-Forward | 5'GATCGCGGACGGGTTGT3' |
| TPT1-Reverse | 5'TTCAGCGGAGGCATTTCC3' |

### 3.4.2. Demethylation treatment with 5'-Aza-2'-deoxycytidine and cDNA quantification by RT-qPCR

Genomic demethylation was induced by treatment with the DNMT inhibitor 5'-Aza-2'-deoxycytidine (AZA, A3656, Sigma Aldrich) at 1µM [64] , in DMEM: F12 medium supplemented with 10% fetal bovine serum (FBS), 2 mM L-glutamine, 1 mM sodium pyruvate, and 1X Antibiotic-Antimycotic mixture, in a humidified atmosphere of 5% CO2 at 37ºC. Cells were plated in ø100-mm culture dishes and passaged at ~80-90% confluence. For experiments, $10^6$ cells were seeded per plate, and the medium containing treatment was replaced every 24 hours. Control cells were incubated for the same periods in the same medium but adding just vehicle (DMSO 0.01% v/v). Samples were collected after 48 and 72 hours of treatment, with all control samples gathered at 72 hours to assess cell viability. Cells were washed with PBS, scraped into 1.5 ml tubes, and centrifuged for 15 seconds, after which the supernatant was discarded, and the pellets were stored at -80°C until further analysis.

RNA was purified following the instructions of the Maxwell RSC Simply RNA Cells kit (Cat. #AS1390). RNA quality was verified by gel electrophoresis, and the concentration was quantified by spectrophotometry at 260/280nm using a NanoDrop ND-1000 (Thermofisher). Samples were then stored at -80°C. RNA was used for cDNA synthesis by reverse-transcription, using the SuperScript IV First-Strand cDNA Synthesis- Reverse Transcriptase kit (Cat:18090050, Invitrogen, Thermo Fisher Scientific), as indicated by the manufacturer. The concentration of template RNA used for reverse transcription was 500ng/µl. The final cDNA products were stored at -20°C.

To quantify the levels of mRNAs in the cell lines subjected to AZA-induced genomic demethylation, an RT-qPCR was conducted with primers for JAK3-ex22-23 and housekeeping genes (*TPT1* and *GAPDH*) for normalization. Conditions per reaction were as follows: 5 µL of LightCycler 480 SYBR Green I Master mix (Roche, Cat.#04887352001) 2x, 1.5 µL of 1/4 diluted cDNA (initial concentration of 500ng/µl), primers at 0.2 µM each, and a final volume of 10 µL. RT-qPCR was performed using a LightCycler 480 II thermocycler, with the following protocol: 1 cycle of 95ºC 10' followed by 40 cycles of 95ºC 10", 60ºC 10" and 72ºC 15", 1 cycle of 95ºC 5", 60ºC 1' and 97ºC. Amplification and melting curves were examined to verify the absence of primer dimers or non-specific products. Quantification was performed using LightCycler® 480 Software with a relative quantification program and standard settings, calculating cycle thresholds (Cts) using the double derivative method. The 2-ΔCT method (**Equation 3.1**) assumes that both the target and the reference gene have similar efficiencies near 100%. First, the CT of the target gene was normalized to that of the reference gene:

$$\Delta C_{T(test)} = C_{T(target,test)} - C_{T(ref,,test)}$$

Afterwards, the expression ratio was calculated:

$2^{-\Delta CT}$ = Normalized expression ratio **(Equation 3.1)**

This approach allows the assessment of how demethylation impacts gene expression, potentially identifying genes whose transcription is directly influenced by promoter methylation and may lead to increased gene expression.

## 3.5. JAK3, STAT3 and phosphorylated STAT3 protein expression

### 3.5.1. Protein extraction

For total protein extraction, $10^6$ cells were seeded in 35 mm dishes (Orange Scientific Braine-l'Alleud, Belgium). Cells were washed with Dulbecco's phosphate-buffered saline (DPBS) (Cytiva; Marlborough, MA, USA) and lysis was carried out using a native lysis buffer (173 mM NaCl, 50 mM Tris-HCl pH 7.4, 5mM EDTA) supplemented with protease inhibitors (Protease Inhibitor cocktail EDTA free, Abcam, Cambridge, UK) and phosphatase inhibitors (Halt Phosphatase Inhibitor Single-use cocktail, Thermo Fisher Scientifics, Waltham, MA, USA). Following this, cells were scrapped from the plates to 1.5mL tubes and incubated for 10 min in ice. Cell membranes were then disrupted, recurring to a UP200s sonicator (Hielscher Ultrasonics GmbH, Teltow, Germany) for 10 s, and cells were centrifuged at 10,000 x g for 10 min at 4 ºC to collect the soluble protein fraction (supernatant). The pellet with the insoluble protein fraction was resuspended in a denaturant lysis buffer (150 mM NaCl, 50 mM Tris-HCl pH 7.4, 0.5% v/v NP-40, 1mM EDTA) supplemented with protease inhibitors (Protease Inhibitor cocktail EDTA free, Abcam, Cambridge, UK) and phosphatase inhibitors (Halt Phosphatase Inhibitor Single-use cocktail, Thermo Fisher Scientifics, Waltham, MA, USA), and samples were sonicated and centrifuged following the same protocol as mentioned above. Samples were kept on ice during the entire process. Proteins were quantified by means of the Bradford assay, using a standard curve with known concentrations of bovine serum albumin (BSA; 0.125 to 2 µg/µL). One µL of samples was incubated with 200 µL of Bradford reagent (Alfa Aesar, Ward Hill, MA, USA) for 10 minutes and read at 595 nm in a Sunrise microplate reader (Tecan, Männedorf, Switzerland).

### 3.5.2. Western Blot

Between 20 and 80 µg of total protein were mixed with 4x loading buffer (250 mM Tris-HCl pH 6.8, 10% w/v sodium dodecyl sulfate (SDS), 40% v/v glycerol, 20% v/v β-mercaptoethanol, 0.008% w/v bromophenol blue). Samples were heated for 5 minutes at 95ºC and then incubated at 4ºC for 5 minutes. Samples were resolved in 10% w/v SDS-polyacrylamide gel electrophoresis at 120V in running buffer (25 mM Tris, 190 mM glycine, 0.1% SDS); and transferred to a nitrocellulose membrane (Cytiva, Marlborough, MA, USA) at 100V for 1 hour in transfer buffer (25 mM Tris, 190 mM glycine, 20% methanol). Transfer efficiency and equal sample loading were confirmed by staining with Ponceau S solution [0,1% w/v Ponceau S (Amresco, Solon, OH, USA), 5% v/v acetic acid and $ddH_2O$ (double-distilled water)]. Ponceau solution was later removed from the membranes by washing them with Tris-Buffered Saline with Tween 20 (TBS-T) (150 mM NaCl, 20 mM Tris pH 7.5, 0.05% v/v Tween 20). Membranes were blocked with 5% w/v skim milk (Nestlé, Vevey, Switzerland) in TBS-T for 1 hour at room temperature and then washed 3 times, 10 minutes each, with TBS-T before incubation with the primary antibodies overnight (**Table 4**). The membranes were then washed 3 times with TBS-T and incubated for 2 hours with the appropriate secondary antibodies (**Table 4).** Next, the membranes were washed 3 times, 10 minutes each, with TBS-T and incubated for 5 min with chemiluminescent Horseradish peroxidase substrate (Thermo Fisher Scientific, Waltham, MA, USA) before imaging in an Amersham Imager 680 RGB (Cytiva, Marlborough, MA, USA).

**Table 4- Antibodies used in Western Blot.** The primary antibodies were diluted in a solution with 5% w/v BSA, 0.05% sodium azide and TBS-T. The secondary antibodies were diluted in 5% w/v skim milk in TBS-T.

| Primary Antibody | Dilution | Manufacturer | Reference |
|---|---|---|---|
| Anti-JAK3 (rabbit) | 1:1000 | Abcam, Cambridge, United Kingdom | #ab45141 |
| Anti-phospho-Y705 STAT3 (mouse) | 1:1000 | Santa Cruz Biotechnology, Dallas, TX, USA | sc-8059 |
| Anti-STAT3 (rabbit) | 1:1000 | Cell Signaling Technology, Danvers, MA, USA | #12640 |
| **Secondary Antibody** | **Dilution** | **Manufacturer** | **Reference** |
| Goat anti-Rabbit IgG (H+L) | 1:10000 | Thermo Fisher Scientific, Waltham, MA, USA | A16096 |
| Goat anti-Mouse IgG (H+L) | 1:10000 | Thermo Fisher Scientific, Waltham, MA, USA | A16066 |

### 3.5.3. Data analysis

Immunoblotting images were analysed using ImageJ software[65] and the resulting quantitative data were tested for statistical significance using GraphPad Prism 9 (GraphPad Software Inc., San Diego, CA, USA). All data was presented as the arithmetic mean ± Standard Error of the Mean (SEM). A One-way ANOVA followed by Tukey test was used for statistical comparison between groups. p-values smaller than 0.05 (*$p < 0.05$; **$p < 0.01$; ***$p < 0.001$) being considered statistically significant.

# IV. Results

## 4.1. Identification of candidate genes within the STAT3 interactome for targeted analysis

### 4.1.1. Expression of JAK genes strongly correlated with STAT3 expression in CRC

A comprehensive computational and bibliography approach (detailed in Materials and Methods section III) yielded a list of 16 genes encoding proteins directly involved in the STAT3 pathway (*ACOX1, BCL2, BCL2L1, CDKN1A, GFAP, IL10, IL2, IL6, IFNG, JAK1, JAK2, JAK3, MCL1, MYC, PIM1, SOCS1, STAT3*). To identify associations at the transcriptional level of STAT3 with the other 16 genes, a co-expression analysis was performed using cBioPortal for Cancer Genomics on the TCGA PanCancer CRC dataset (n=524 samples). Specifically, mRNA co-expression was assessed across 524 samples of CRC, with Spearman's correlation coefficients and p-values calculated for all human protein-encoding genes. The p-values were corrected for multi-hypothesis testing using the false discovery rate (FDR) method, yielding corrected p-values named q-values. Out of the 16 genes, 11 exhibited a statistically significant (FDR-corrected q-value < 0.001) positive association with *STAT3* expression, three exhibited moderately significant associations (FDR-corrected q-value < 0.01), one a borderline significant correlation (q-value=0.018), and only one did not exhibit a statistically significant correlation (*PIM1*, q-value = 0.59) (**Table 5**).

**Table 5- Correlation of mRNA expression of genes associated with the *STAT3* pathway.** Data obtained from TCGA PanCancer colorectal dataset using cBioportal. The table lists gene name and location ordered according to Spearman's correlation coefficients along with the corresponding p-values and the FDR-corrected q-values.

| Correlation with STAT3 | Cytoband | Spearman's Correlation | p-Value | q-Value | Sig. |
|---|---|---|---|---|---|
| *JAK1* | 1p31.3 | 5,77E-01 | 6,84E-48 | 6,80E-44 | *** |
| *JAK3* | 19p13.11 | 3,98E-01 | 2,39E-21 | 1,41E-19 | *** |
| *JAK2* | 9p24.1 | 3,63E-01 | 9,67E-18 | 2,85E-16 | *** |
| *MCL1* | 1q21.2 | 3,38E-01 | 1,67E-15 | 3,27E-14 | *** |
| *BCL2* | 18q21.33 | 3,35E-01 | 3,09E-15 | 5,66E-14 | *** |
| *IFNG* | 12q15 | 3,13E-01 | 2,26E-13 | 2,96E-12 | *** |
| *IL10* | 1q32.1 | 2,61E-01 | 1,23E-09 | 8,28E-09 | *** |
| *SOCS1* | 16p13.13 | 2,48E-01 | 9,25E-09 | 5,35E-08 | *** |
| *IL6* | 7p15.3 | 2,38E-01 | 3,45E-08 | 1,81E-07 | *** |
| *GFAP* | 17q21.31 | 1,94E-01 | 8,05E-06 | 2,78E-05 | *** |
| *IL2* | 4q27 | 1,59E-01 | 2,73E-03 | 5,89E-03 | ** |
| *ACOX1* | 17q25.1 | 1,57E-01 | 3,03E-04 | 7,86E-04 | *** |
| *CDKN1A* | 6p21.2 | 1,51E-01 | 5,21E-04 | 1,29E-03 | ** |
| *PIM1* | 6p21.2 | 2,90E-02 | 5,06E-01 | 5,91E-01 | N. S |
| *MYC* | 8q24.21 | -1,13E-01 | 9,32E-03 | 1,80E-02 | * |
| *BCL2L1* | 20q11.21 | -1,39E-01 | 1,37E-03 | 3,15E-03 | ** |

The mRNA expression of the 17 selected genes was compared in MSI vs MSS CRCs. MSI was determined using the MSISensor Score[66], a measure to classify MSI tumours provided by cBioportal. Tumours with a MSI score > 3.5 were considered MSI (n=74) while tumours with MSI score < 3.5 were considered MSS (n=450). The analysis also included *MLH1* as a positive control since downregulation of this gene due to promoter methylation is one of the typical characteristics of MSI tumours. The results revealed that 11 of the 17 genes exhibited differential expression in MSI vs MSS tumours ($p < 0.01$ after multi-hypothesis correction). The differences were in both directions, i.e. some genes were more expressed in MSI than in MSS tumours, while others exhibited the reverse trend (**Figure 4.1**).

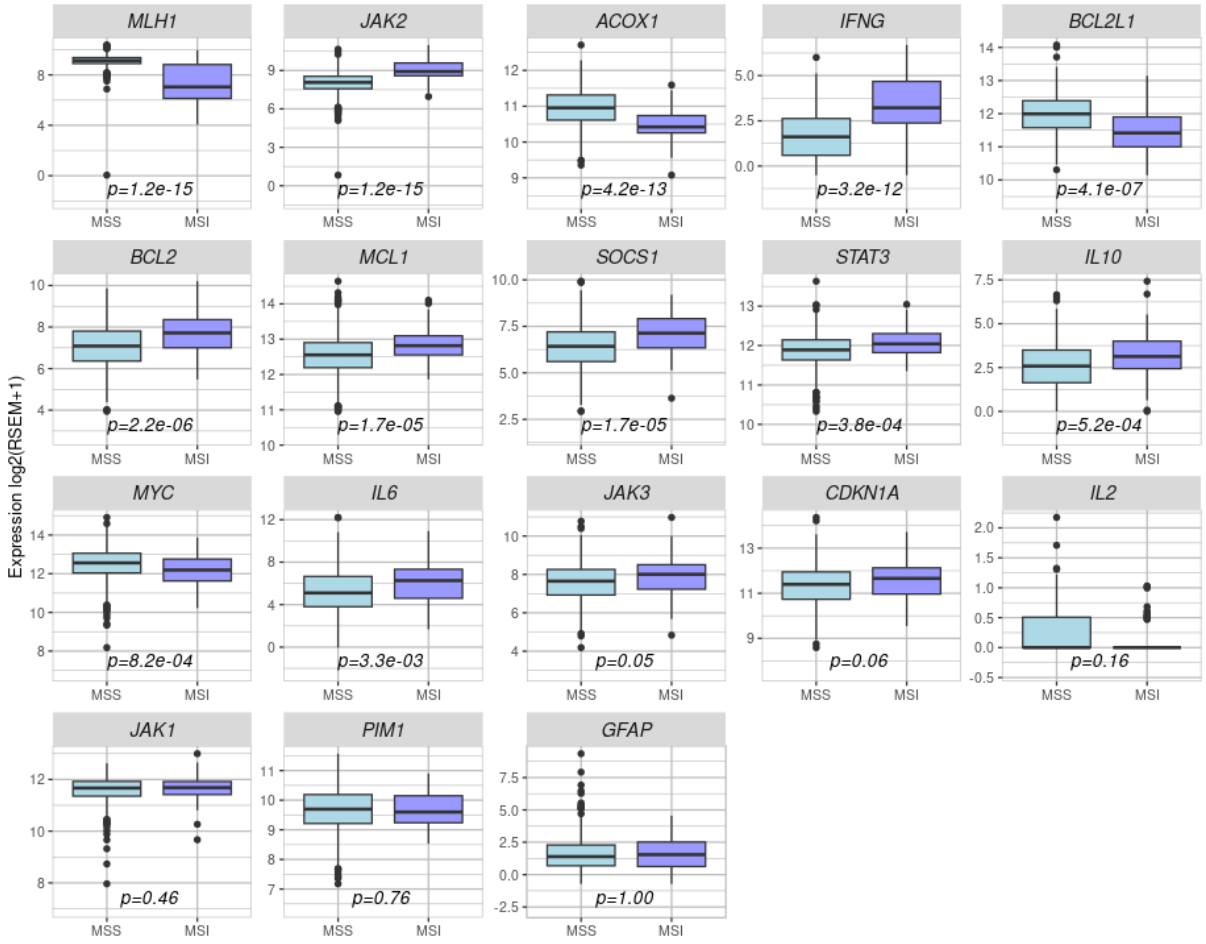


**Figure 4.1- mRNA expression levels of MLH1 and the 17 selected STAT3-related genes in MSS and MSI CRCs.** Data from the TCGA PanCancer colorectal dataset, obtained through cBioportal. p-values were calculated by t-test and corrected for multi-hypothesis testing using the FDR method.

### 4.1.2. Methylation analysis with TCGA Wanderer

The initial methylation analysis of the 17 STAT3-related genes was conducted using TCGA Wanderer (http://maplab.cat/wanderer), a tool that allows visualization of methylation of CpG sites interrogated by the Illumina HM450K methylation arrays in tumours, in comparison to histologically normal tissue. The analysis was performed separately for colon adenocarcinoma (COAD) and rectum adenocarcinoma (READ), because the TCGA did not provide a single unified CRC dataset. This analysis facilitated the determination of hypo- or hypermethylated CpG sites along the sequence of the selected gene, primarily focusing on hypermethylation taking place in the promoter regions.

The methylation of the *STAT3* promoter was first examined for colon (**Figure 4.2-A)** and for rectum

(**Supplementary Figure SD.1-A)** adenocarcinomas. Both analyses revealed very similar methylation patterns, with no significant methylation differences between tumour and normal tissues. The only probes showing significant hypermethylation within the CpG islands of *STAT3* were cg05548912 and cg13467672. However, these probes were located within the gene body and not in the promoter region. Therefore, their methylation status was not expected to greatly affect gene expression.

Of all the studied genes (**Table 6**), *JAK3* demonstrated the most promising results in this phase (**Figure 4.2-B**). All probes (cg05315206, cg10357657, cg04916091, cg05635754) located in the CpG islands of the promoter showed hypermethylation in tumours when compared to normal tissues. Probes cg10357657, cg04916091 showed a p-value < 0.01. The analysis was replicated for all selected genes, and annotations were based on plot visualizations. Although other genes exhibited hypermethylation, only those with a higher Spearman's correlation, a significant p-value (< 0.05) (**Table 5**), and a greater number of hypermethylated probes near the promoter were selected for further analyses.

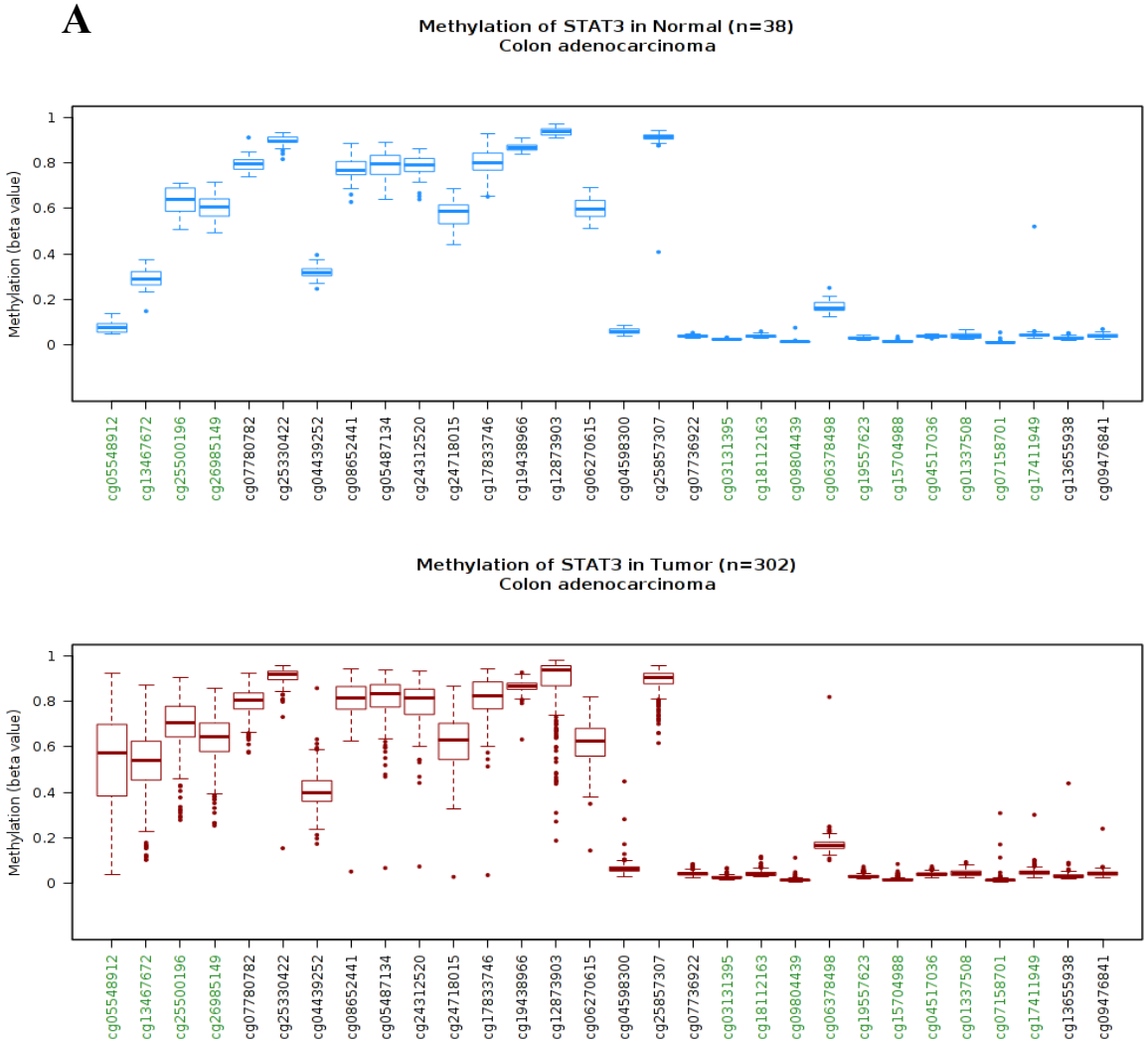

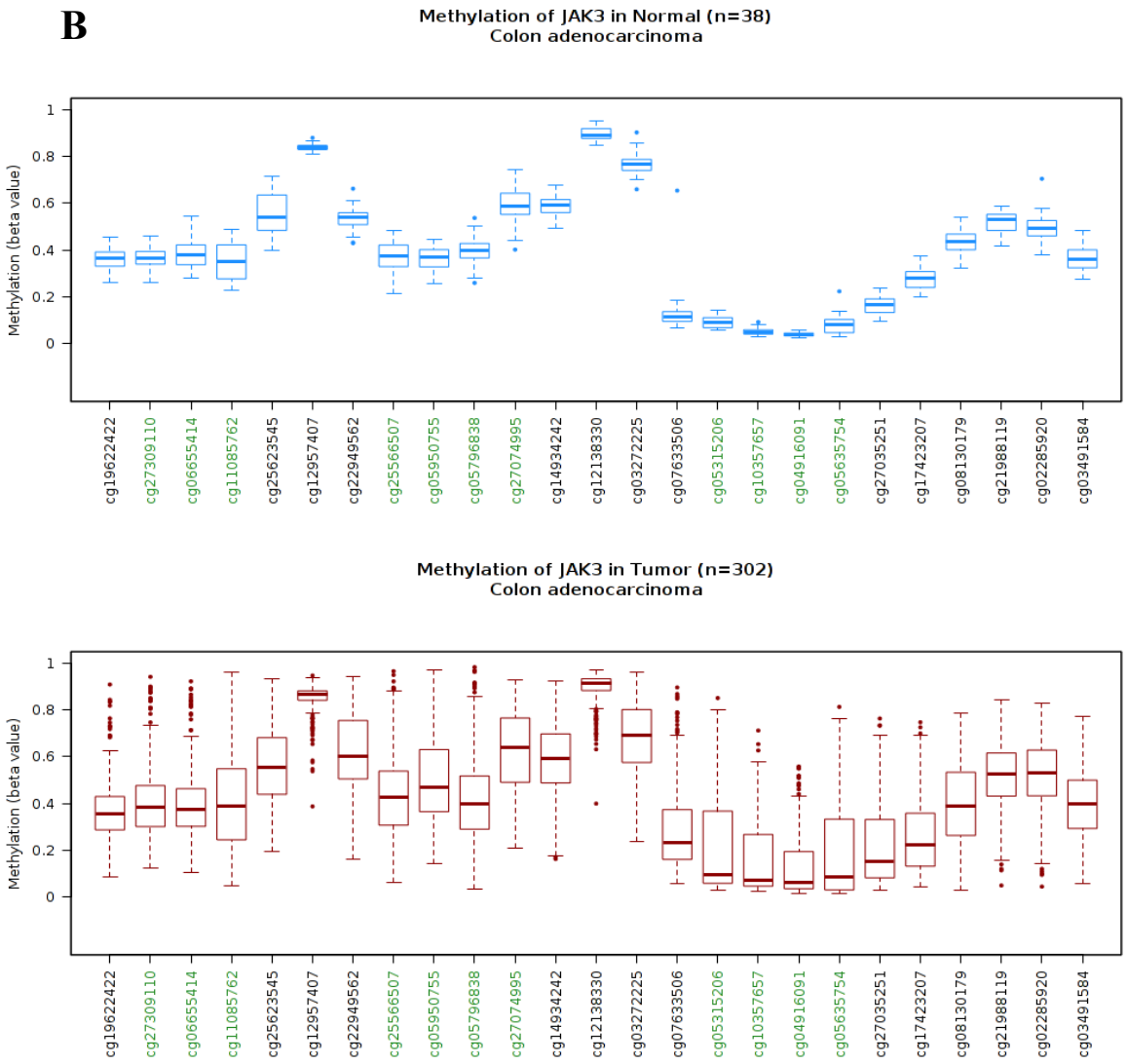


**Figure 4.2- Methylation of *STAT3* and *JAK3* in colon adenocarcinomas and adjacent histologically normal tissue.** A- *STAT3* locus, chr17:40441000-40541000, containing 30 CpG sites interrogated by Illumina HM450K arrays. B- JAK3 locus, chr19:17937000-17959000, containing 25 CpG sites interrogated by Illumina HM450K arrays. The probes are represented in the x-axis ordered according to their genomic location, but with uniform spacing between consecutive probes to avoid overlaps of the boxplots. Methylation level in the y-axis, ranging from 0 (completely unmethylated) to 1 (completely methylated). The probes highlighted in green are in CpG islands. In both cases, the transcription direction is from right to left, and therefore the promoter-associated probes are in the right part of the graphs. Image obtained from TCGA Wanderer.[60]

**Table 6- Methylation status of *STAT3*-related genes.** This table presents the methylation status of *STAT3*-related genes in TCGA colon adenocarcinoma (COAD) and rectum adenocarcinoma (READ) data sets. The methylation status is categorized as follows: **M** for methylated, **NM** for non-methylated, **Hypo** for hypomethylated (less methylation in tumours than in normal tissues), and **Hyper** for hypermethylated (more methylation in tumours than in normal tissues). The notation **(-)** reflects a minimal probe count of either hyper or hypomethylated probes. The presence of CpG islands is marked with "Yes" or "No," where "Yes". The location of these CpG islands in relation to the promoter region is also indicated, along with the number of available probes for each gene in the designated regions.

| Gene symbol | Methylation status | | CpG islands | In promoter region | Number of probes |
|---|---|---|---|---|---|
| | COAD | READ | | | |
| ***IL2*** | M | NM | No | No | 1 |
| ***IL6*** | M-Hypo | M-Hypo | No | No | 11 |
| ***IL10*** | M-Hypo | M-Hypo | No | No | 4 |
| ***IFNG*** | M-Hypo | M-Hypo | No | No | 5 |
| ***JAK1*** | M | M | Yes | No | 23 |
| ***JAK2*** | M-hyper (-) | M | Yes | Yes | 15 |
| ***JAK3*** | M-Hyper | M-Hyper | Yes | Yes | 25 |
| ***CDKN1A*** | M-Hypo | M-Hypo | Yes | No | 28 |
| ***BCL2*** | M-Hyper (-) | M-Hypo (-) | Yes | Yes | 39 |
| ***MCL1*** | NM | NM | Yes | No | 18 |
| ***BCL2L1*** | M-Hyper (-) | M-Hyper (-) | Yes | Yes | 19 |
| ***PIM1*** | M-Hyper (-) | M-Hyper (-) | Yes | No | 10 |
| ***MYC*** | M-Hyper (-) | M-Hyper (--) | Yes | Yes | 40 |
| ***ACOX1*** | M- Hypo | M-Hypo (-) | Yes | Yes | 27 |
| ***GFAP*** | M- Hypo and Hyper | M- Hypo and Hyper | Yes | No | 21 |
| ***SOCS1*** | M-Hyper | M-Hyper (-) | Yes | Yes | 19 |
| ***STAT3*** | M-Hyper (-) | M-Hyper (-) | Yes | Yes | 30 |

### 4.1.3. Confirmation of methylation status of the selected genes in an independent CRC cohort

After determining the methylation status of the genes of interest in the TCGA datasets (COAD and READ), I reassessed their methylation on an in-house dataset of 82 CRCs analysed with Illumina Methylation EPIC arrays. The EPIC arrays provided a higher resolution data compared to the Illumina HM450K arrays used by the TCGA. The microarray data quality control and processing were previously performed by other members of the laboratory. They created an R script that generated heatmap plots of the methylation per sample and interrogated CpG sites (e.g. Figures 4.3. and 4.4), and association plots showing the correlation of the level of methylation in every CpG with different clinical and mutational parameters (i.e. age, gender, location, MSI, mutations in *TP53, KRAS, BRAF*, **Figure 4.5**). As illustrated in **Figure 4.3**, STAT3 exhibited very low levels of methylation in the promoter region in all analysed CRC samples, suggesting that the genetic expression and transcription are not controlled by methylation. For the other genes analysed, the methylation patterns provided further insights, although the majority showed no significant methylation variations in the promoter region.

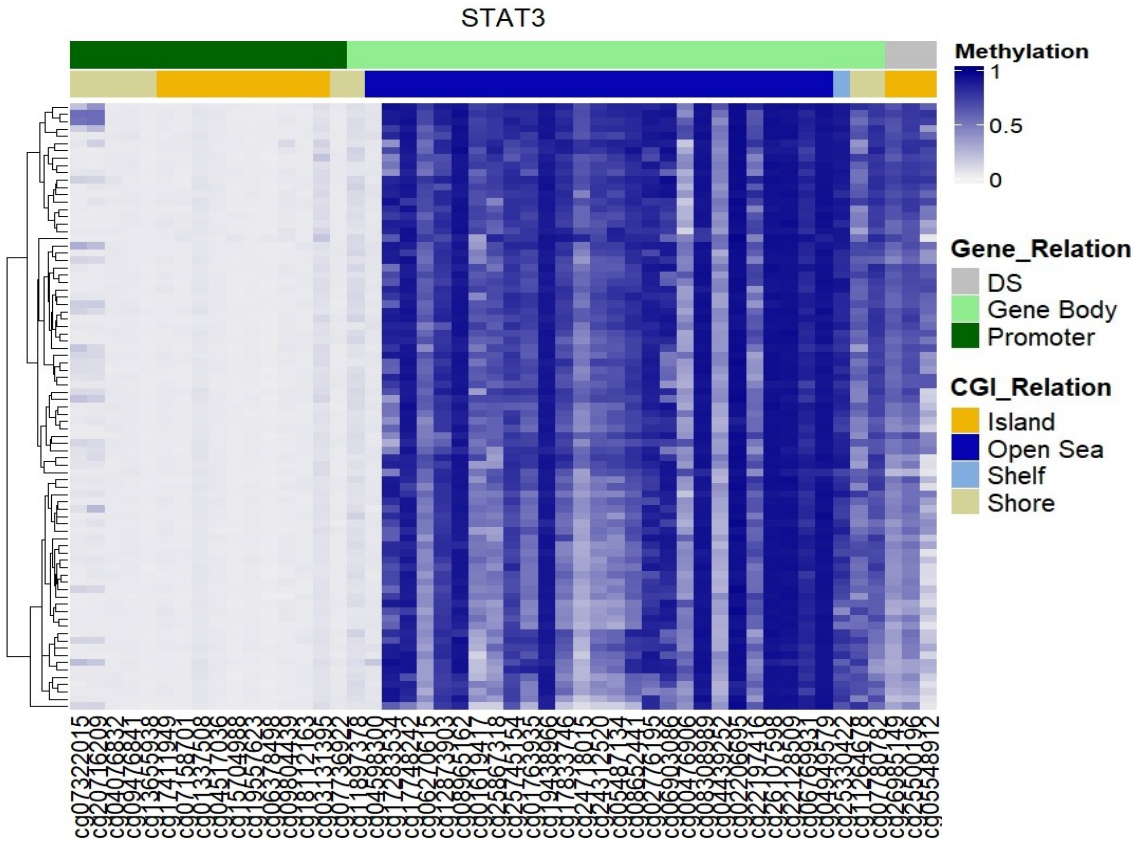


**Figure 4.3- Methylation status of STAT3 in CRC tissue.** Hierarchical heatmap of levels of methylation obtained from the database based on 82 samples/patients with CRC and adjacent normal tissue obtained with Infinium Methylation EPIC Bead Chip array. In the x-axis is shown the probes, and in the y-axis the hierarchical clustering of differentially methylated 82 samples. In CGI relation, shores, in other words, regions up to 2 kb from CpG island; shelves, in other words, regions from 2 to 4 kb from CpG island and open sea, in other words, the rest of the genome. In gene relation, DS stands for downstream of the gene body. Probes considered more relevant are in a CpG island (in orange) in the gene's promoter region (in dark green). No considerable methylation was found in STAT3. Methylation is evaluated according to their β-value, that ranges from 0 (Unmethylated) in white to 1 (Methylated) in dark blue.

In the 82 CRCs analysed with the Illumina EPIC arrays, *JAK3* exhibited a pattern of methylation (**Figure 4.4**) similar to that previously observed in the COAD/READ TCGA datasets (**Figure 4.2-B)**. Probes in the promoter-associated CpG islands showed variable levels of methylation, indicative of hypermethylation in some – but not all – tumours. Of note, although this CpG island is only interrogated by two probes, this does not imply they are the only CpG sites in that region. None of the probes in the *JAK3* promoter associated with patient gender, age, tumour location of tumour lymphocytic infiltration. The probes in the promoter-associated CpG island correlated with MSI and *BRAF* mutations, with a p-value < 0.01 (**Figure 4.5)**. This is not unexpected, since tumours with *BRAF* mutations are associated with MSI and with extensive promoter hypermethylation of many genes in CRCs.[67] However, the previous analysis on the TCGA data did not identify any significant association between MSI status and *JAK3* expression (**Figure 4.1**). Additionally, a relationship with *KRAS* mutation in other probes located in the promoter region but outside the CpG island was observed.

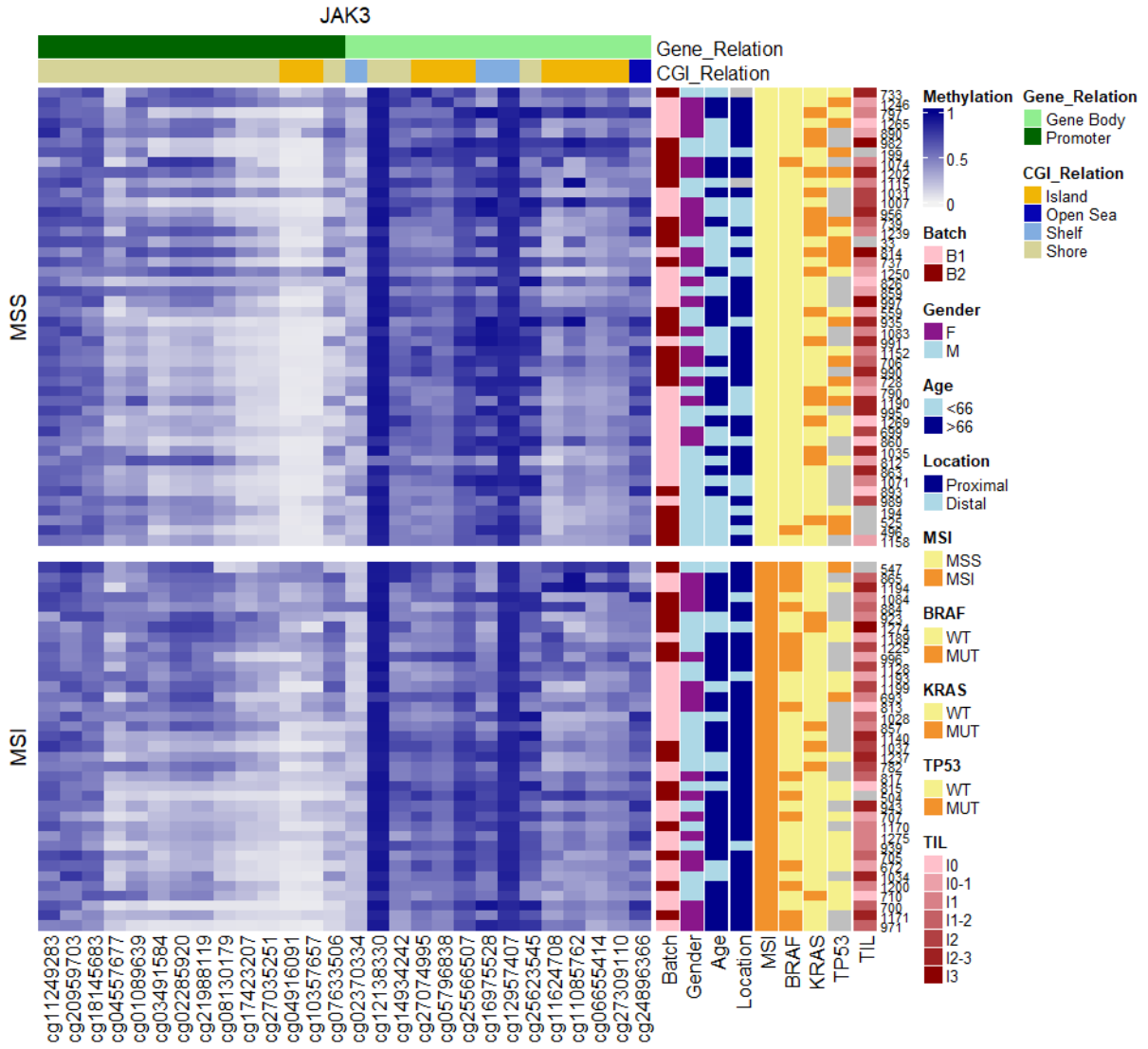


**Figure 4.4- Methylation status of *JAK3* in CRC tissue.** Heatmap of methylation obtained from the database based on 82 CRCs analysed with Infinium Methylation EPIC BeadChip arrays. Clinicopathological data is shown (i.e. gender, age, and tumour location proximal CRC was defined as tumours from the cecum to the splenic flexure, while distal CRC was defined as tumours from the descending colon to the rectum), MSI, KRAS, BRAF and TP53 mutation analysis. WT: wild type. MUT: mutant. TIL refers to the level of tumour infiltrating lymphocytes, analysed by hematoxylin and eosin staining. Samples are divided in MSS (top) and MSS (bottom). Methylation of every interrogated site (columns) is represented according to their β-value, which ranges from 0 (Unmethylated) in white to 1 (Methylated) in dark blue. In both groups, MSS and MSI, there are substantial variations in methylation in the JAK3 promoter region. Probes cg04916091 and cg10357657 are located in the area of most relevance (CpG island in the promoter in orange), and show an average level of methylation, with the highest levels of methylation corresponding to MSI.

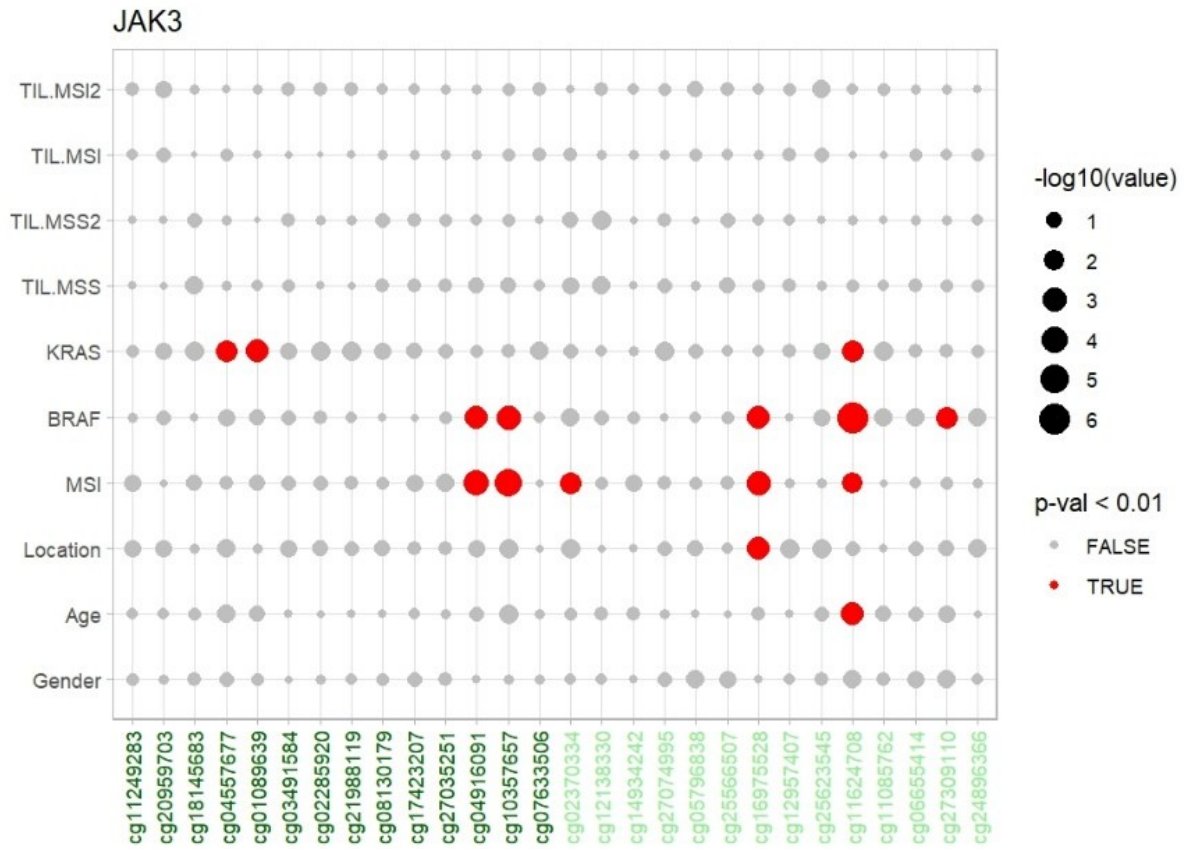


**Figure 4.5- Association analysis of *JAK3* methylation levels across clinical and genetic factors.** Every dot in the plot represents the *p*-value of univariate ANOVA analyses of the probes of JAK3 (x-axis) as a dependent variable and a parameter (y-axis) as an independent variable. The size of the dots is proportional to the -log10 of the *p*-value. The colour of the dots indicates the level of statistical significance, red for p-values below 0.01 and grey for non-significant associations (p-value >0.01). Rows represent factors. TIL indicates lymphocyte infiltration, measured separately in MSS and MSI tumours, and with 2 different methods to calculate the association. This classification was performed for a different project concurrently ongoing in the laboratory, and it is not relevant to the content of this Master. Specific genetic mutations (*KRAS, BRAF*), MSI status, tumour location and demographic details like age, and gender, are also shown. Columns denote different probes, labelled on the x-axis. The circle size reflects the statistical significance of the association between *JAK3* methylation and each factor.

## 4.2. Assessment of JAK3 promoter methylation across CRC cell lines

### 4.2.1. JAK3 exhibited high methylation status in CRC

The methylation status of the *JAK3* promoter region was evaluated in five CRC cell lines and one small intestine cancer cell line, derived from different patients, and representing diverse molecular backgrounds. These cell lines exhibit varying mutations that may influence DNA methylation and gene expression patterns (**Table 8**). The small intestine cell line HuTu-80 was added to the analysis as an internal control and reference point.

Two independent PCR reactions were initially designed to analyse the *JAK3* promoter region. The first set of primers, PB-456 and PB-457, produced an amplicon of 417 bp, while the second set, PB-458 and PB-459, was expected to yield a product of 265 bp. However, the first set failed to produce a unique product of the expected size. Then, it was designed a new set of primers, PB-466 and PB-467, to cover the whole region with a different strategy (**Figure 4.6**). The primers were used in the following pairs: PB-458 and PB-466, amplifying an expected 467bp product, and PB-467 and PB-457, with a 233bp amplicon.

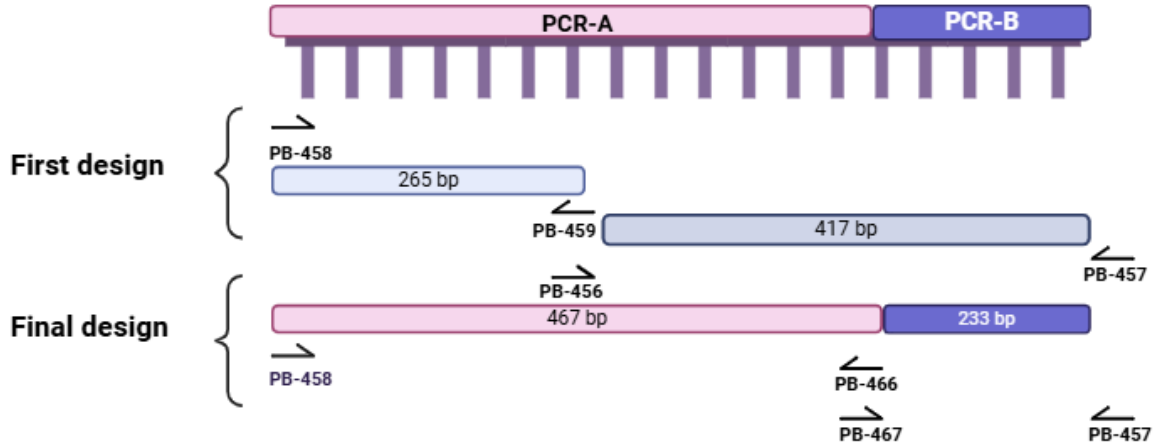


**Figure 4.6- Design of primers for *JAK3* promoter bisulfite sequencing.** First design corresponds to PB-458 and PB-459, along with PB-556 and PB-457. The final design: PCR-A generated with PB-458 and PB-466, and PCR-B with PB-467 and PB-457.

The methylation status of the 19 CpG sites interrogated by PCR-A and the 17 CpG sites interrogated by PCR-B was determined by bisulfite sequencing, as detailed in Materials and Methods (Section III). At least 6 independent sequences were analysed by cell line and PCR (**Figure 4.7**). LS174T was identified as the CRC cell line with the lowest methylation (60,99% of methylation), while HCT116 exhibited the highest level of methylation (94,75% of methylation) (**Figure 4.8**). Overall, the small intestine cancer cell line (HuTu-80) was the least methylated, particularly in the region interrogated by PCR-B, with 51,79% of interrogated sites being methylated. Thus, *JAK3* is highly methylated in CRC cell lines, with more than half of the interrogated sites showcasing methylation.

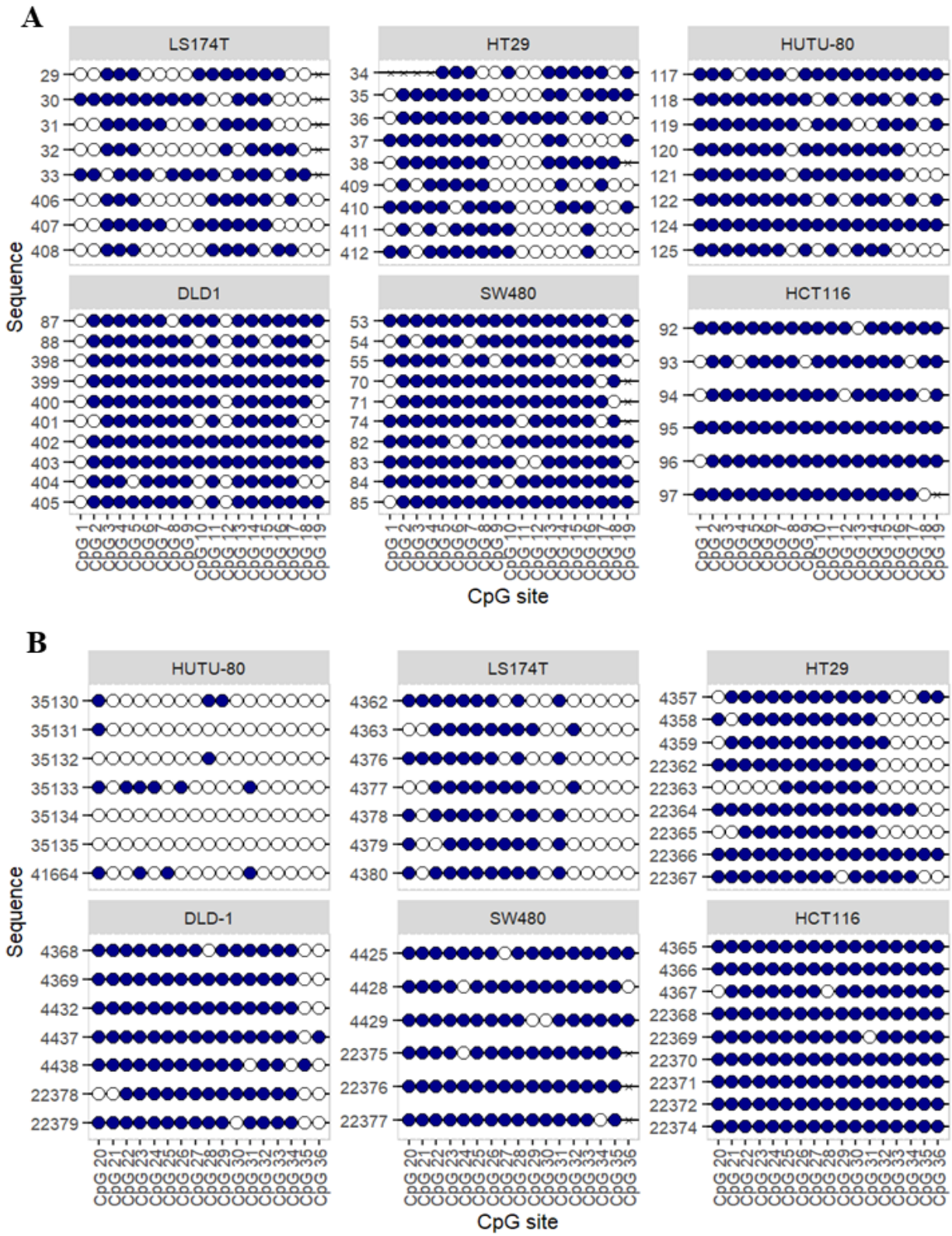


**Figure 4.7- Methylation status of *JAK3* promoter in cell lines**. Obtained by bisulfite sequencing. A- Methylation status of the *JAK3* PCR-A, which spans 467 base pairs and includes 19 CpG sites: B- Methylation status of JAK3 PCR-B, covering 233 base pairs and containing 17 CpG sites. Every circle corresponds to a CpG site. Blue circles represent methylated CpG sites, and white circles represent unmethylated sites. Each number represents a distinct independently sequenced clone (clone sequence ID).

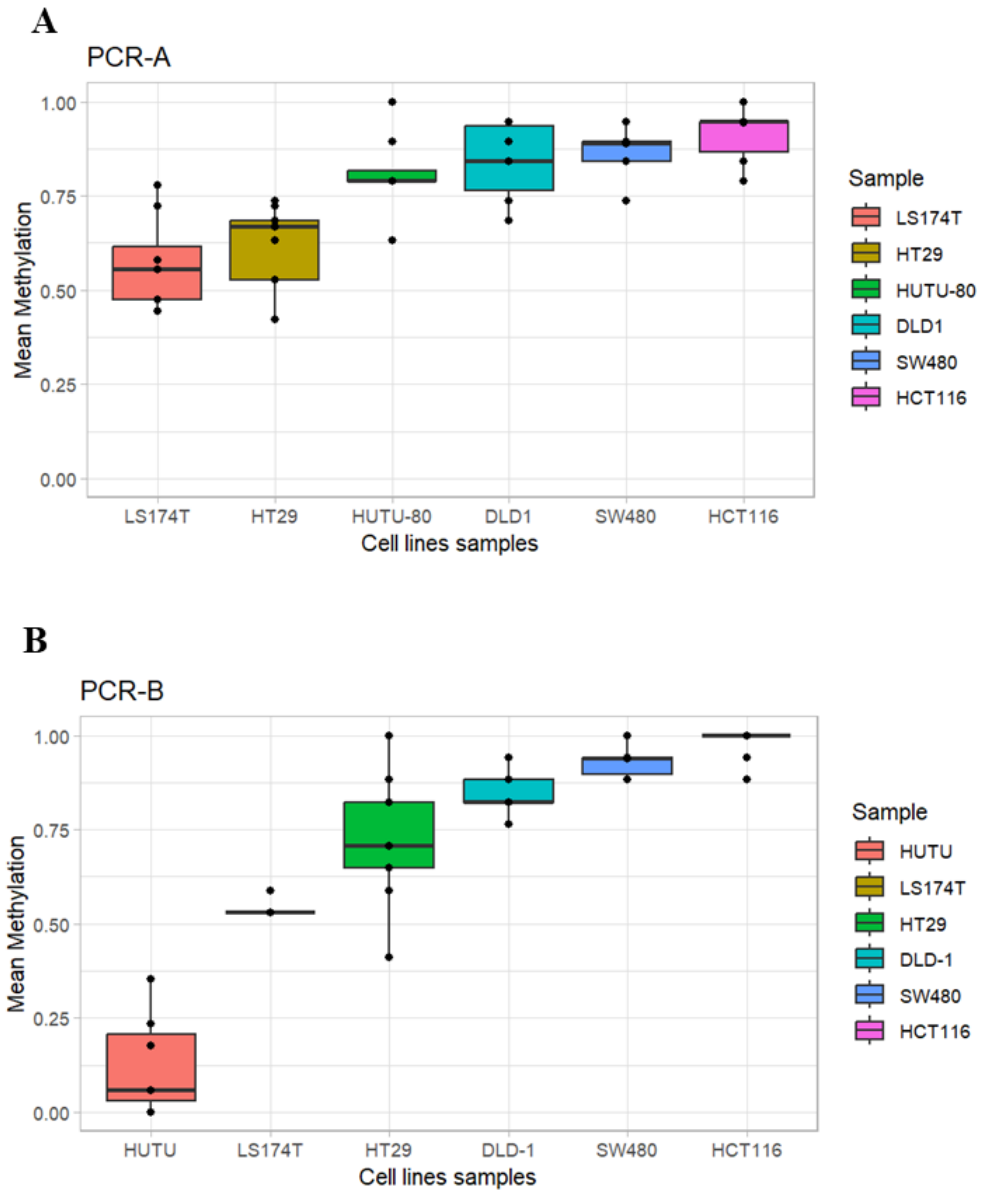


**Figure 4.8- *JAK3* methylation of each CpG site of CRC and small intestine cancer cell lines.** Two specific regions were analysed by PCR: PCR-A, covering 467 base pairs (bp), and PCR-B, covering 233 bp. The mean methylation for each PCR region was calculated from a minimum of six sequences, obtained by colony PCR using DNA from the cell lines DLD-1, HCT116, HT-29, Hutu-80, LS174T, and SW480. A- mean methylation of 19 CpG sites for PCR-A; B- mean methylation of 17 CpG sites corresponding to PCR-B.

The analysis of the mean methylation of the *JAK3* promoter region covered by the PCR-A revealed two groups of samples. All cell lines exhibited mean methylation values above 50%, but LS174T and HT29 exhibited lower levels of methylation (below 75%) than the rest of the cell lines (all pairwise comparisons with p-value < 0.001, **Table 7**), The methylation level in LST174T and HT29 was very similar (p-value=0.97, **Table 7**). The other 4 cell lines exhibited higher levels of methylation (above 75%), with no statistically significant differences among them (all p-values > 0.4, **Table 7**). The *JAK3* promoter region covered by PCR-B exhibited a very different profile. In this case, the lowest methylation level was found in HuTu-80 (methylation < 0.25), with statistically significant differences

with all the CRC cell lines (all p-values < 0.001, **Table 7**). LS174T exhibited a lower level of methylation, slightly above 50%, and significantly different than the methylation in the rest of the CRC cell lines (all p-values < 0.01).

**Table 7- Pairwise comparisons of methylation in JAK3 promoter regions covered by PCR-A and PCR-B.** Mean methylation differences were analysed by one-way ANOVA followed by Tukey's honestly significant difference test. Comparisons are ordered according to the absolute value of the difference in means (diff). The lower (lwr) and upper (up) 95% confidence intervals are indicated. The p-values were corrected for multi-hypothesis testing.

**Comparisons for mean methylation value in PCR-A**

| | Comparison | diff | lwr | upr | p.value |
|---|---|---|---|---|---|
| 1: | LS174T-HCT116 | -0.34 | -0.50 | -0.18 | 2.3e-06 |
| 2: | HT29-HCT116 | -0.30 | -0.46 | -0.14 | 1.5e-05 |
| 3: | SW480-LS174T | 0.30 | 0.16 | 0.44 | 2.1e-06 |
| 4: | LS174T-DLD1 | -0.26 | -0.41 | -0.12 | 2.5e-05 |
| 5: | SW480-HT29 | 0.26 | 0.12 | 0.40 | 1.6e-05 |
| 6: | LS174T-HUTU-80 | -0.24 | -0.39 | -0.09 | 3.8e-04 |
| 7: | HT29-DLD1 | -0.23 | -0.36 | -0.09 | 2.0e-04 |
| 8: | HUTU-80-HT29 | 0.20 | 0.05 | 0.35 | 2.7e-03 |
| 9: | HUTU-80-HCT116 | -0.10 | -0.27 | 0.06 | 0.43 |
| 10: | HCT116-DLD1 | 0.07 | -0.08 | 0.23 | 0.71 |
| 11: | SW480-HUTU-80 | 0.06 | -0.08 | 0.21 | 0.78 |
| 12: | SW480-HCT116 | -0.04 | -0.20 | 0.12 | 0.97 |
| 13: | LS174T-HT29 | -0.04 | -0.18 | 0.11 | 0.97 |
| 14: | SW480-DLD1 | 0.04 | -0.10 | 0.17 | 0.97 |
| 15: | HUTU-80-DLD1 | -0.03 | -0.17 | 0.12 | 0.99 |

**Comparisons for mean methylation value in PCR-B**

| | Comparison | diff | lwr | upr | p.value |
|---|---|---|---|---|---|
| 1: | HUTU-80-HCT116 | -0.85 | -1.01 | -0.70 | 1.2e-13 |
| 2: | SW480-HUTU-80 | 0.80 | 0.64 | 0.97 | 1.2e-13 |
| 3: | HUTU-80-DLD-1 | -0.72 | -0.88 | -0.56 | 1.3e-13 |
| 4: | HUTU-80-HT29 | -0.61 | -0.76 | -0.45 | 3.4e-13 |
| 5: | LS174T-HCT116 | -0.44 | -0.59 | -0.29 | 1.6e-09 |
| 6: | LS174T-HUTU-80 | 0.41 | 0.25 | 0.57 | 4.2e-08 |
| 7: | SW480-LS174T | 0.39 | 0.22 | 0.56 | 3.1e-07 |
| 8: | LS174T-DLD-1 | -0.31 | -0.47 | -0.15 | 1.5e-05 |
| 9: | HT29-HCT116 | -0.25 | -0.39 | -0.11 | 8.5e-05 |
| 10: | SW480-HT29 | 0.20 | 0.04 | 0.36 | 7.4e-03 |
| 11: | LS174T-HT29 | -0.19 | -0.35 | -0.04 | 5.7e-03 |
| 12: | HCT116-DLD-1 | 0.13 | -0.02 | 0.28 | 0.12 |
| 13: | HT29-DLD-1 | -0.12 | -0.27 | 0.04 | 0.22 |
| 14: | SW480-DLD-1 | 0.08 | -0.09 | 0.25 | 0.70 |
| 15: | SW480-HCT116 | -0.05 | -0.21 | 0.11 | 0.93 |

A correlation analysis was performed to study the relationship between individual CpG sites and the average methylation of the region (**Figure 4.9**). CpG sites 18, 19, 21, 22, 32, and 33 showed strong positive correlations with the average methylation, indicating that these sites most closely reflect the overall methylation pattern. Conversely, CpG sites 1, 3, 8, 20, and 28 exhibited the strongest negative correlations, suggesting that their methylation tends to deviate inversely from the mean. This analysis

identified the most informative CpG sites for understanding the methylation dynamics in the studied region, with strongly correlated sites potentially serving as markers of the *JAK3* promoter.

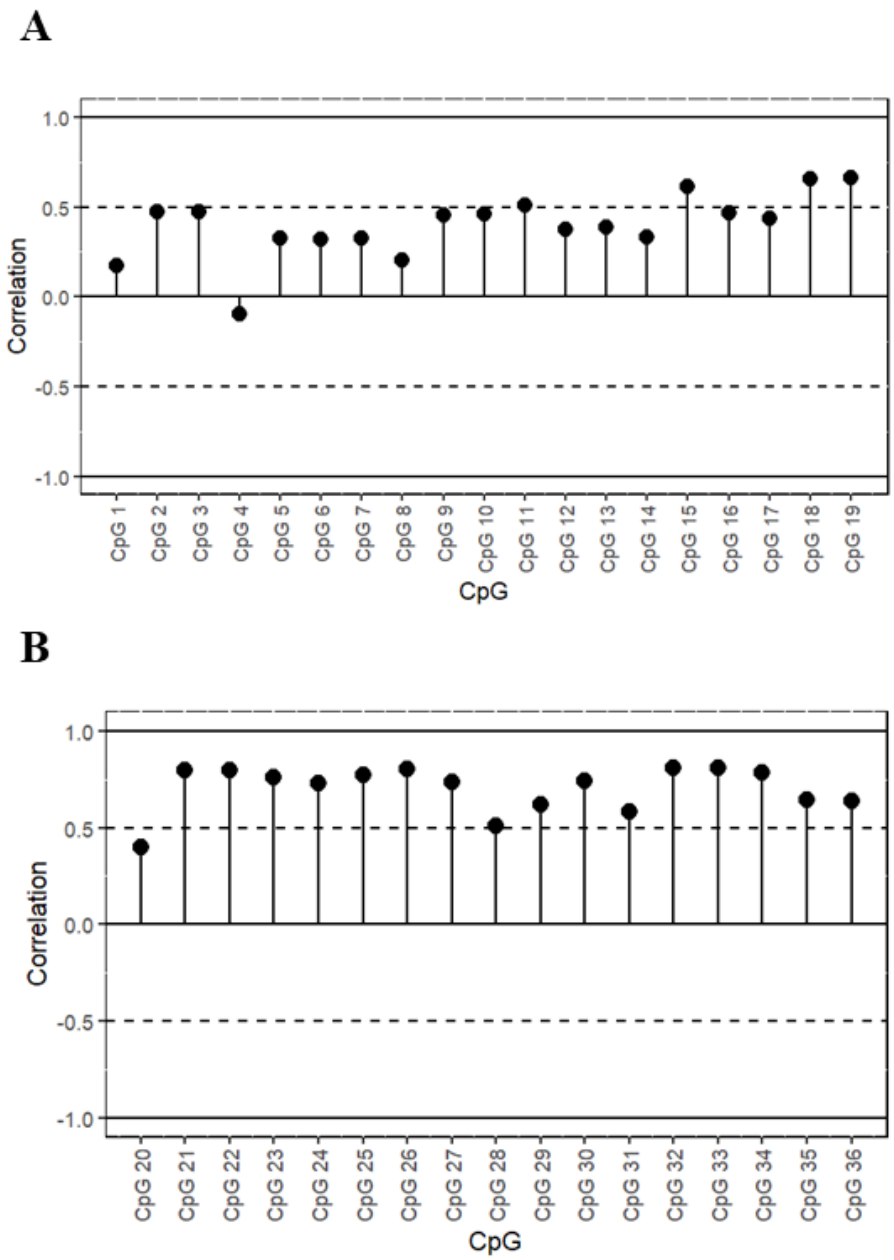


**Figure 4.9- Correlation of each CpG site of CRC and small intestine cancer cell lines.** It shows correlation between each CpG site and the mean methylation across all interrogated sites. Correlation ranges from -1 (negative correlation) to +1 (positive correlation). A- refers to 19 CpG sites in PCR-A; B- refers to 16 CpG sites in PCR-B.

### 4.2.2. JAK3 promoter methylation vs molecular characteristics of CRC cell lines

It was performed an exploratory analysis of the associations between *JAK3* promoter methylation, and the molecular characteristics of the CRC cell lines (**Table 8**). This analysis was unavoidable very low powered, due to the reduced number of cell lines analysed (n=5). Nevertheless, it revealed a strong positive correlation between the methylation level in the regions covered by PCR-A and PCR-B (r=0.94, p-value=0.016). No significant differences in methylation were found associated with *TP53* mutations, MSI status, or CIMP (all p-values > 0.6). No comparison for *KRAS* mutations was performed because

all cell lines, except HT29, harboured mutant *KRAS*. Notably, cell lines with *BRAF* mutations (HT29 and LS174T), exhibited lower levels of methylation in the region covered by PCR-A (59.1% vs 87.4%, p-value=$2.5x10^{-3}$, t-test), and also in the region covered by PCR-B (63.5% vs 92%), although in the latter region, the comparison did reach the statistical significance threshold (p=0.17, t-test). Notably, the cell line with the lowest methylation level, i.e. LS174T, is MSI, CIMP-, and carries both *KRAS* and *BRAF* mutations, a combination that is typically mutually exclusive. [68] Moreover, the mutation in *BRAF* (D211G) is atypical, found just in one large intestine sample according to the Catalog Of Somatic Mutations In Cancer (COSMIC).[69] The D211G mutation is very rare and of unclear effect. LS174T is an MSI cell line that accumulates thousands of mutations, many without clear phenotypic effect. This might underlie the concomitant mutations in KRAS and BRAF in this cell line.

**Table 8- Summary of mutation status in CRC critical genes in CRC cell lines.** Mean methylation of each cell line per PCR and the Standard deviation was added. Mutation status was adapted from Berg et al[70]

| Cell line | Methylation PCR-A | Methylation PCR-B | *TP53* | *KRAS* | *BRAF* | MSI | CIMP |
|---|---|---|---|---|---|---|---|
| DLD-1 | 83.7 ± 10.4% | 84.9 ± 5.7% | p.S241F | p.G13D | wt | MSI | CIMP+ |
| HCT116 | 91.2 ± 7.9% | 98.0 ± 4.2% | wt | p.G13D | wt | MSI | CIMP+ |
| HT29 | 61.0 ± 12.3% | 73.2 ± 17.4% | p.R273H | wt | p.V600E; p.T119S | MSS | CIMP+ |
| LS174T | 57.3 ± 12.0% | 53.8 ± 2.2% | wt | p.G12D | p.D211G | MSI | CIMP- |
| SW480 | 87.2 ± 6.1% | 93.0 ± 4.4% | p.R273H; p.P309S | p.G12V | wt | MSS | CIMP- |

## 4.3. JAK3 mRNA expression analysis in colorectal and small intestine cancer cell lines

### 4.3.1. Basal JAK3 mRNA expression was very low in CRC cell lines and did not respond to 5-AZA-2-deoxycytidine

The Human Protein Atlas indicated very low transcription of *JAK3* in virtually all CRC cell lines, with undetectable expression in DLD-1, HCT116, HT29, SW480 and LS180 (a syngeneic sister cell line of LS174T) (**Figure 4.10**).

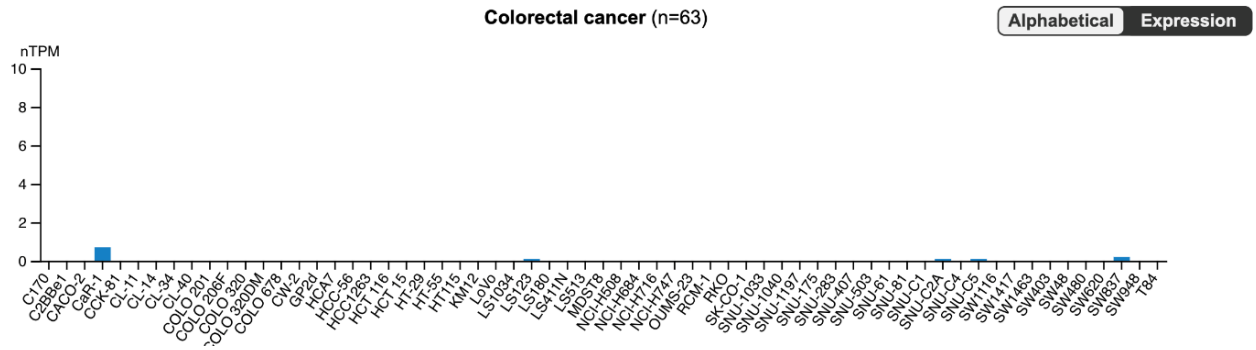


**Figure 4.10- JAK3 mRNA expression in CRC cell lines.** The data was generated by Genentech, and available at the Human Protein Atlas. The expression is represented by nTPM (normalized transcripts per million).

To experimentally determine *JAK3* mRNA expression in our laboratory, the primers were designed to amplify the mRNA at exons 22-23, which belongs to the catalytic JH1 domain and thus is present in all functional JAK3 products. The relative mRNA expression of *JAK3* was quantified by RT-qPCR (see

Materials and methods, Section III) in reference to two housekeeping genes, i.e. *GAPDH* and *TPT-1*. To divide the workload, the experiments were distributed in two batches. Every batch included SW480 and HT29 to verify the absence of a significant batch effect. All cell lines exhibited very low levels of *JAK3* mRNA, around three to four levels of magnitude lower than the housekeeping genes. The cell lines with the highest *JAK3* mRNA expression were HCT116 (Target/Ref = $5.12x10^{-4}$) and Hutu-80 (Target/Ref = $8.36x10^{-4}$). In contrast, LS174T (Target/Ref = $3.21x10^{-5}$) and HT29 (Target/Ref = $7.16x10^{-5}$) cell lines showed even lower expression by one order of magnitude.

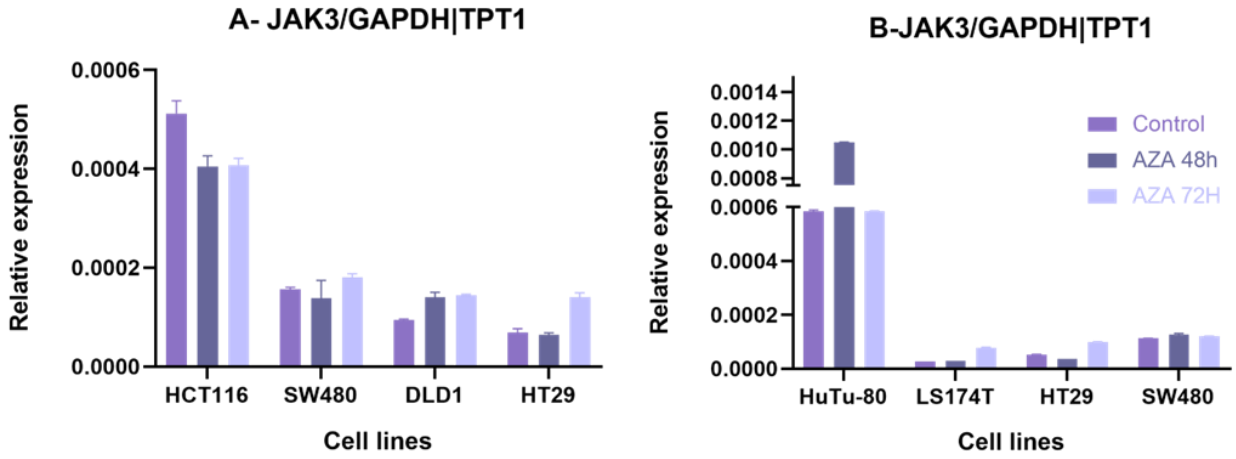


**Figure 4.11- Relative expression analysis of JAK3 mRNA levels.** mRNA expression of JAK3 was evaluated with qPCR in cell lines both treated with 5'-Aza-2'-deoxycytidine for 48h and 72h time points and untreated (control). The analysis was divided into two batches with 2 of the cell lines (SW480, HT29) repeated in both as an internal control.

It was then studied whether pharmacologically induced genome demethylation restored *JAK3* expression. To induce genome-wide demethylation, the DNA methyltransferase inhibitor AZA was used. AZA treatment was evaluated after 48 and 72 hours of treatment since demethylation requires at least one mitosis to occur. However, AZA treatment did not exhibit any drastic effect on *JAK3* mRNA expression in any of the cell lines, except for HuTu-80 at 48h, but not at 72h (**Figure 4.11**).

## 4.4. Protein expression studies of JAK3, pSTAT3 and STAT3 in CRC cell lines

### 4.4.1. JAK3 is undetected in CRC and small intestine cancer cell lines

The levels of JAK3, STAT3, and Y705-phosphorylated STAT3 (pSTAT3) were evaluated in DLD-1, HCT116, HT29, HuTu-80, LS174T, SW480 cell lines. JAK3 is primarily localized in the cytosol, according to The Protein Atlas Database, but we were unable to detect JAK3 in the soluble fraction of total protein extracts from HCT116 and LS174T cells. Bearing in mind the canonical pathway of JAK activation, it was hypothesized that JAK3 could be membrane-bound and precipitate with the insoluble fraction. However, we were also unable to detect JAK3 in the insoluble fraction of DLD-1, HT29, LS174T, and HuTu-80 cells (**Figure 4.13- A** to **C**).

The JAK3 antibody was initially tested in CFBE, a bronchial epithelial cell line (provided by the Cystic Fibrosis Research Lab, BioISI), since JAK3 is commonly present in lung tissue.[71] However, JAK3 expression was not detected in this cell line (**Figure 4.13**). Consequently, a cell line with higher and more reliable expression of JAK3 was required. THP-1, a human leukaemia monocytic cell line (kindly provided by Dr Margarida Gama-Carvalho, RNA Systems Biology Lab, BioISI), was

subsequently and successfully used as a positive control, since JAK3 is predominantly expressed in hematopoietic tissues.[71] (**Figure 4.12)**.

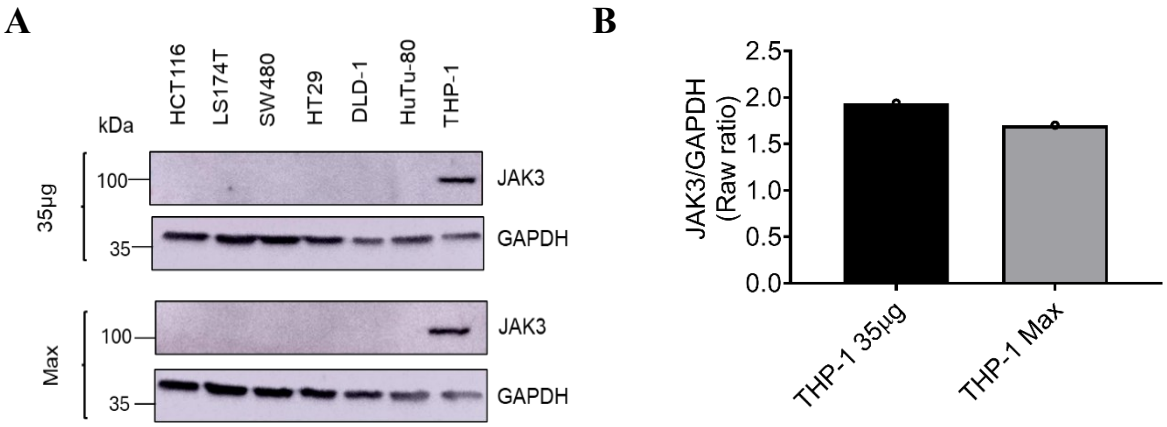


**Figure 4.12- Validation of JAK3 antibody**. A- Western blots of the CRC cell lines with positive control (THP-1), with 2 different concentrations of protein, the first with 35µg and below the maximum amount of protein from each, going from 40 to 60 µg (n=1). B-quantification of JAK3 relative expression to GAPDH

### 4.4.2. STAT3 and phosphorylated STAT3 were detected in CRC cell lines

Among the CRC cell lines, HT29 had the highest and the most significant STAT3 total expression levels (**Figure 4.13-D**). Regarding the levels of phosphorylated STAT3 in Y705 (**Figure 4.13-E**), HT29 continues to present high levels, along with SW480 and HCT116 with a high amount of phosphorylation in this residue, but DLD-1 is much less expressed. Regarding the insoluble fraction of the proteins (**Figure 4.13-F and H**), SW480 has a much higher amount of pSTAT3, considering their total STAT3 expression levels. For the rest of the cell lines, HT29 showed a rather low amount of pSTAT3 in the insoluble fraction, a similar trend to the one seen in the soluble fraction.

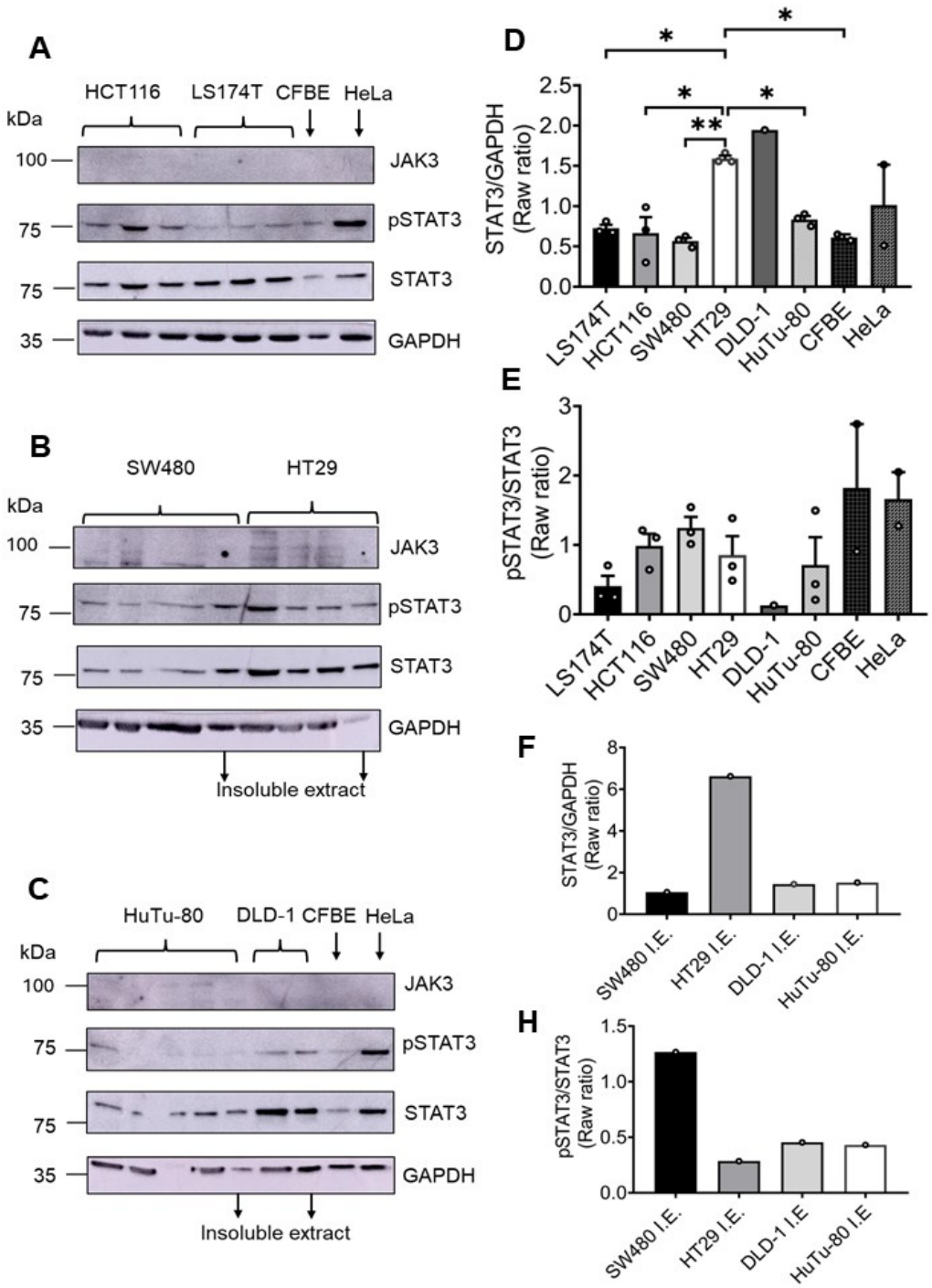


**Figure 4.13- JAK3, pSTAT3 and STAT3 levels in soluble and insoluble protein extracts from CRC and small intestine cancer cell line.** A, B and C-Total protein extractions from HCT116, LS174T, SW480, HT29, DLD-1 and Hutu-80 were carried out with native lysis buffer and for the insoluble protein fraction of SW480, HT29, DLD-1 and HuTu-80 were obtained with denaturant lysis buffer and analysed by Western blot. The concentrations of protein were quantified and calculated for maximum load ranging from 35 to 70 µg/µL (n=3 except for DLD-1, which was n=1). The Human CF Bronchial Epithelial cell line (CFBE) (concentration of protein=35 µg/µL) was used as a potential positive control for JAK3 expression, and HeLa cells (concentration of protein=20 µg/µL) were used as a positive control for STAT3 and pSTAT3 expression. D-Quantification of protein expression of total STAT3 in relation to GAPDH; with HT29 and DLD-1 having the highest of the CRC cell lines, no significances from DLD-1 were illustrated due to lack of replicates (n=1); E-Quantification of pSTAT3 (Y705) levels normalized versus STAT3 levels; F and H- Quantification of insoluble protein fraction expression in both STAT3 relative to GAPDH and the subpopulation of phosphorylated STAT3

# V. Discussion

The present work aimed at analysing genetic and epigenetic alterations in the *JAK/STAT3* pathways in CRC. Initially, the study was focused on the promoter of *STAT3*. The computational analyses, based on over 400 TCGA CRC primary tumours analysed with Illumina HM450K arrays, and 82 CRCs from our laboratory collection analysed with Illumina EPIC arrays, indicated that *STAT3* did not exhibit significant promoter methylation in CRC (**Figures 4.2 and 4.4**). This result contrasted with findings from prior pan-cancer studies (He et al., 2023)[72], which reported statistically significant differences in *STAT3* promoter methylation between tumour and normal tissues. On a more detailed inspection, their results reported small differences in very low methylation values (with a maximum of 0.06). These small differences in methylation, albeit statistically significant, are very unlikely to have any physiological relevance and might explain the discrepancy with our findings. Based on our results, *STAT3* promoter methylation in CRC may not be as pronounced or functionally relevant as in other cancer types. Consequently, we aimed to identify another potential participant within the *STAT3* pathway that would be dysregulated in CRC by promoter hypermethylation.

Given the well-established link between CRC development and progression[73] and methylation alterations,[73] we examined various genes within the *STAT3* pathway that had a strong connection to the primary gene of interest (**Tables 5 and 6**). From the explored *JAK/STAT3* pathways, many factors were found to be involved in key cellular processes such as cell growth (*Cyclin D1, c-Myc*), anti-apoptosis (*Bcl-xL, PIM1*), angiogenesis (*VEGF*), and differentiation (*GFAP*). Moreover, *STAT3* was identified as a significant effector in inflammatory bowel disease, particularly by increasing the frequency of Th17 cells associated with immune regulation. Most of the selected genes did not exhibit promoter hypermethylation in CRC, with some of the upstream effectors even showing hypomethylation (e.g. *IL-6, IL-10, IFNG* and *ACOX1*)[39,74]. *JAK3* promoter was found to be hypermethylated in a substantial proportion of CRC samples (**Table 6 and Figure 4.2**) and therefore was selected for further investigation. The difference in methylation between normal tissues and primary tumours suggested a potential role for *JAK3* promoter methylation in colorectal carcinogenesis, possibly leading to gene silencing and decreased *JAK3* expression.[75] Since JAK3 is an upstream effector in the STAT3 pathway, we reckoned that downregulation of JAK3 could potentially impact STAT3 phosphorylation and consequently the phenotype of cancer cells. In our tumour collection, we found substantial variability in *JAK3* promoter methylation among tumours (**Figure 4.4**), regardless of their MSI status. A more detailed analysis of the differences in methylation according to different clinical and mutational parameters, revealed that methylation of some of the CpG interrogated by the Illumina EPIC arrays, was associated with MSI and *BRAF* mutations. In particular, the CpG sites interrogated by the array probes cg04916091 and cg10357657, exhibited the most pronounced difference in MSI vs MSS (**Figure 4.4**), yielding the most statistically significant values (**Figure 4.5**). These probes are located within the promoter-associated CpG island of *JAK3*, and thus their methylation status is very likely to be involved in transcription modulation. Of note, *JAK3* promoter hypermethylation has been reported in other cancers, such as urothelial bladder cancer, where it was linked to low-grade, non-invasive tumours and favourable prognosis.[76]

The *JAK3* promoter-associated CpG island is located 5.3 kb downstream of the transcriptional start site, is 1.3 kb in length, and contains 88 CpG sites, of which only 2 were interrogated by the Illumina EPIC arrays (data obtained from the ENSEMBL genome browser). To study the methylation status of this CpG island in a much higher resolution we employed bisulfite sequencing, a technique that offers single-nucleotide resolution of the methylation status of the targeted sequence. Bisulfite sequencing, however, presented some technical challenges, particularly due to the primer design constraints (**Figure 4.6**). Primers should typically be longer than standard PCR primers, ranging from 26 to 35 bases, to compensate for the reduced sequence complexity after bisulfite conversion. The optimal GC content for

these primers is around 30%, as the original sequence often contains at least 60% G+C before treatment. It is crucial to avoid including CpG sites in the primers, when possible, as these can introduce bias; if unavoidable, CpG sites should be placed at the 5' end of the primer and synthesized with mixed bases (Y for C/T, R for G/A) at the cytosine position. Primers should be designed to have melting temperatures above 50°C, preferably above 60°C, to ensure specificity. Finally, the amplicon size should generally be kept between 200-500 bases due to DNA fragmentation during bisulfite treatment.

Several sets of PCR primers were designed to amplify the most CpG-dense region of the *JAK3* promoter-associated CpG island. The final design encompassed two sets of primers, amplifying a sequence of 467bp encompassing 19 CpG sites (PCR-A), and an adjacent sequence of 233bp encompassing 17 CpG sites (PCR-B). The bisulfite-sequencing analysis of these sequences in 5 CRC cell lines revealed widespread hypermethylation (**Figure 4.7 and 4.8**), with LS174T showing the lowest level among CRC lines at 60% of CpG sites. This contrasted with the observation in primary CRCs, where some tumours exhibited methylation while others did not (**Figures 4.2 and 4.4).** The difference in methylation pattern in cell lines *versus* primary tumours might reflect a fundamental difference between CRC cells cultured *in vitro* and those growing *in vivo*. Epigenetic alterations due to adaptation to *in vitro* culturing are, in fact, not uncommon. This phenomenon has been well-documented in previous studies[77]. A simpler explanation is that the number of cell lines used in the study is insufficient to cover the epigenetic variability observed in primary tumours.

The study also allowed to identify which CpG sites within the *JAK3* promoter sequence were the most informative of the average region methylation (**Figure 4.9**). This is important because these sites could be used in other methylation analysis techniques beyond bisulfite sequencing, such as pyrosequencing[78], Methylation-specific qPCR (MS-qPCR), and Combined Bisulfite Restriction Analysis (COBRA).[79] These techniques allow the processing of a larger number of samples more easily, faster and cost-effectively, but they require the identification of the most informative CpG sites to obtain an accurate measure of the methylation in the region of interest.

To determine if promoter methylation affected mRNA expression in the cell lines used, the cells were treated with AZA, a hypomethylating agent that inhibits DNA methylation activity by trapping and degrading DNA methyltransferases producing genome-wide demethylation after mitosis. Despite its pleiotropic effect, AZA treatment is widely used to investigate the causal effect of promoter methylation in gene expression, considering the lack of techniques to directly and specifically demethylate a target sequence. mRNA expression was specifically analysed in exons 22-23, located in the JH1 catalytic/kinase domain of *JAK3*.[80] Our results revealed a low basal expression level across the cell lines, consistent with previous studies **(Figure 4.10)** and high levels of promoter methylation. However, HCT116 exhibited the highest *JAK3* expression, despite being the cell line with the highest promoter methylation. AZA treatment did not have any dramatic effect on *JAK3* transcription (**Figure 4.11**). In fact, the most methylated cell line, HCT116, exhibited a decrease in JAK3 expression after AZA treatment. A possible explanation is that the HCT116 does not express transcriptional activators, or that it expresses some transcriptional repressors, targeting the *JAK3* promoter. Thus, despite the promoter being accessible after DNA demethylation, transcription is not activated. There might be other indirect effects due to the pleiotropic response to AZA. A similar phenomenon was observed by Moghadasi et al[81], in microRNA expression of MOLT4 and Jurkat cells (T lymphoblast and lymphocyte, respectively), where they made a correlation between the decreasing levels of expression after AZA treatment, correlating with increased p53 expression and activation of an apoptotic pathway. This process requires functional p53, which is present in HCT116 cells and could explain in part the observed behaviour (**Table 8**).

In contrast, LS174T, SW480, and HT29 exhibited a slight increase in *JAK3* mRNA following AZA treatment. The expression increase, however, was not very dramatic, and certainly much smaller than

the observed in other genes that are known to be silenced by hypermethylation in cancer[82]. Similarly to HCT116, the lack of clear response to AZA treatment might be due to the lack of essential transcriptional activators, the presence of transcriptional repressors, or more complex and indirect effects due to the pleiotropic response to AZA. Altogether, these experiments failed to demonstrate a clear effect of *JAK3* methylation and gene expression, at least in the studied promoter-associated CpG island.

Despite the low mRNA expression identified in the previous experiments, we sought to investigate whether the low *JAK3* mRNA levels could be sufficient to produce observable levels of JAK3 protein. Protein expression studies were conducted not only on JAK3 but also on STAT3 and phosphorylated STAT3 (pSTAT3) (**Figure 4.12**). The protein expression of JAK3 was not detected in any of the CRC or small intestine cancer cell lines. The antibody effectiveness was confirmed using cell extracts from THP-1, a leukaemia cell line known to express the protein (**Figure 4.11).** Similarly, no JAK3 expression was detected in HeLa or CFBE cell lines. This finding was unexpected, particularly considering the article Lin et al [27] which demonstrated JAK3 protein expression in SW480 using Western blotting. Additionally, the presence of the γc chain in SW480 and HT29, which is necessary for JAK3-mediated signalling, was reported.[27] But despite using protein extracts with the maximum possible protein load in a Western blot, JAK3 was still undetectable in any of the cell lines studied. These results are consistent with previous research on JAK3 expression in non-lymphoid and non-myeloid cells, such as in DLD-1, where no JAK3 expression was observed.[83] Conversely, Shareef et al.[84] explored the relation between JAK3 and STAT3 in CRC tumour samples, along with different types such as adenomas and ulcerative colitis, both JAK3 and pJAK3 were immunoreactive in 45 samples of CRC analysed (93% and 89% respectively). A correlation between JAK3 and low-grade dysplasia and colectomy samples with more advanced stages was also stipulated.

Significant expression differences of STAT3, particularly in HT29 to the rest of the explored cell lines were detected. Regarding the subpopulation of phosphorylated STAT3 (pSTAT3), the SW480 showed a higher expression not only in the soluble but also in the insoluble fraction, but there was no significance detected. Contradicting the findings of other researchers [27,84], it was not possible to infer a relation between JAK3 and STAT3, suggesting a more nuanced interaction. The discrepancy between JAK3 methylation patterns and protein expression suggests that additional regulatory mechanisms may be involved. These could include histone modifications, which can work in concert with DNA methylation to regulate gene expression, or post-transcriptional regulation by microRNAs.[85] It also raises the possibility of compensatory mechanisms within the JAK/STAT3 pathway. Other JAK family members, such as JAK1 or JAK2, might compensate for the loss of JAK3 function, maintaining STAT3 signalling. Especially, JAK1 could have this behaviour given that it can cooperate with JAK3 in signalling through γc-containing receptors.[86] This redundancy in the pathway could explain why STAT3 activation persists despite JAK3 hypermethylation and lack of protein expression.

**Limitations of the study and future directions**

One of the limitations of our study was that all the selected CRC cell lines exhibited *JAK3* promoter methylation, at least in the analysed CpG island, and thus they did not reflect the variability in methylation that we observed in the primary CRC samples. Although it is possible that epigenetic silencing of JAK3 is not a relevant alteration in CRC, the fact that it undergoes somatic hypermethylation in a large proportion of primary tumours suggests that this alteration has a phenotypic effect providing some selective advantage. Studying this effect has been hampered by the fact that none of the cell lines expressed JAK3, which was consistent with the fact that they have promoter methylation, and more importantly by the fact that demethylation with AZA failed to restore transcription, suggesting that other factors, genetic or epigenetic, are also involved in the absence of transcriptional activity of *JAK3*. Including other CRC cell lines that express *JAK3*, such as CaR-1 or SW837 (**Figure 4.10**) could facilitate future investigations on the role of JAK3 silencing in CRC. Unfortunately, these cell lines were

not available in our laboratories. Alternatively, JAK3 expression could be studied in primary tumour samples with and without *JAK3* promoter methylation, using either qPCR or immunohistochemistry. Those studies would require more time and effort given the complexities of working with human tumour samples but would benefit from the observations and techniques set up during this research project.

In the future, it also would be interesting to analyse additional candidate genes in the STAT3 pathway that might have a strong effect on the pathway, such as *SOCS1,* a known inhibitor that showed hypermethylation in the computational analysis, both in available online data but also with in-house arrays.

# VI. Conclusions

- *STAT3* does not undergo promoter methylation in CRC patient samples, suggesting that direct regulation of *STAT3* through promoter methylation is unlikely in this context.
- *JAK3* promoter undergoes somatic hypermethylation in a substantial proportion of primary CRCs
- *JAK3* exhibited high levels of promoter methylation across 5 CRC cell lines. mRNA and protein expression are very low and uncorrelated with the promoter methylation levels.
- The response to AZA treatment, an inhibitor of methyltransferases, varied among the cell lines, implying that epigenetic regulation of gene expression through methylation is context dependent.
- Despite the absence or very low expression of JAK3, we still observe phosphorylation of STAT3 at different levels in the analysed CRC cell lines, indicating that other kinases could be involved in the constitutive activation of STAT3.
- These findings suggest that JAK3 may not play a direct role in modulating STAT3 activity through protein expression in the studied cell lines, contrary to previous reports. This discrepancy highlights the complexity of signalling pathways in cancer and the need for further verification of findings.

# VII. References


1. Cancer Today. https://gco.iarc.who.int/today/.
2. Okugawa, Y., Grady, W. M. & Goel, A. Epigenetic Alterations in Colorectal Cancer: Emerging Biomarkers. *Gastroenterology* **149**, 1204-1225.e12 (2015).
3. Lao, V. V. & Grady, W. M. Epigenetics and Colorectal Cancer. *Nat. Rev. Gastroenterol. Hepatol.* **8**, 686–700 (2011).
4. Mármol, I., Sánchez-de-Diego, C., Pradilla Dieste, A., Cerrada, E. & Rodriguez Yoldi, M. J. Colorectal Carcinoma: A General Overview and Future Perspectives in Colorectal Cancer. *Int. J. Mol. Sci.* **18**, 197 (2017).
5. Jasperson, K. W., Tuohy, T. M., Neklason, D. W. & Burt, R. W. Hereditary and Familial Colon Cancer. *Gastroenterology* **138**, 2044 (2010).
6. Guinney, J. *et al.* The consensus molecular subtypes of colorectal cancer. *Nat. Med.* **21**, 1350–1356 (2015).
7. Ogino, S. *et al.* CpG island methylator phenotype (CIMP) of colorectal cancer is best characterised by quantitative DNA methylation analysis and prospective cohort studies. *Gut* **55**, 1000–1006 (2006).
8. Mohelnikova-Duchonova, B., Melichar, B. & Soucek, P. FOLFOX/FOLFIRI pharmacogenetics: The call for a personalized approach in colorectal cancer therapy. *World J. Gastroenterol. WJG* **20**, 10316–10330 (2014).
9. Cunningham, D. *et al.* Cetuximab monotherapy and cetuximab plus irinotecan in irinotecan-refractory metastatic colorectal cancer. *N. Engl. J. Med.* **351**, 337–345 (2004).
10. Hurwitz, H. *et al.* Bevacizumab plus irinotecan, fluorouracil, and leucovorin for metastatic colorectal cancer. *N. Engl. J. Med.* **350**, 2335–2342 (2004).
11. Xie, Y.-H., Chen, Y.-X. & Fang, J.-Y. Comprehensive review of targeted therapy for colorectal cancer. *Signal Transduct. Target. Ther.* **5**, 1–30 (2020).
12. Mellman, I., Coukos, G. & Dranoff, G. Cancer immunotherapy comes of age. *Nature* **480**, 480–489 (2011).
13. Galon, J. & Bruni, D. Approaches to treat immune hot, altered and cold tumours with combination immunotherapies. *Nat. Rev. Drug Discov.* **18**, 197–218 (2019).

14. Pagès, F. *et al.* International validation of the consensus Immunoscore for the classification of colon cancer: a prognostic and accuracy study. *The Lancet* **391**, 2128–2139 (2018).

15. Di Giorgio, A., Botti, C., Tocchi, A., Mingazzini, P. & Flammia, M. The influence of tumor lymphocytic infiltration on long term survival of surgically treated colorectal cancer patients. *Int. Surg.* **77**, 256–260 (1992).

16. Heregger, R. *et al.* Unraveling Resistance to Immunotherapy in MSI-High Colorectal Cancer. *Cancers* **15**, 5090 (2023).

17. Mlecnik, B. *et al.* Integrative Analyses of Colorectal Cancer Show Immunoscore Is a Stronger Predictor of Patient Survival Than Microsatellite Instability. *Immunity* **44**, 698–711 (2016).

18. Xue, C. *et al.* Evolving cognition of the JAK-STAT signaling pathway: autoimmune disorders and cancer. *Signal Transduct. Target. Ther.* **8**, 1–24 (2023).

19. Wang, H.-Q. *et al.* STAT3 pathway in cancers: Past, present, and future. *MedComm* **3**, e124 (2022).

20. Philips, R. L. *et al.* The JAK-STAT pathway at 30: Much learned, much more to do. *Cell* **185**, 3857–3876 (2022).

21. Hu, X., Li, J., Fu, M., Zhao, X. & Wang, W. The JAK/STAT signaling pathway: from bench to clinic. *Signal Transduct. Target. Ther.* **6**, 1–33 (2021).

22. Liongue, C., Ratnayake, T., Basheer, F. & Ward, A. C. Janus Kinase 3 (JAK3): A Critical Conserved Node in Immunity Disrupted in Immune Cell Cancer and Immunodeficiency. *Int. J. Mol. Sci.* **25**, 2977 (2024).

23. Barcia Durán, J. G. *et al.* Endothelial Jak3 expression enhances pro-hematopoietic angiocrine function in mice. *Commun. Biol.* **4**, 1–14 (2021).

24. Lodi, L. *et al.* STAT3-confusion-of-function: Beyond the loss and gain dualism. *J. Allergy Clin. Immunol.* **150**, 1237-1241.e3 (2022).

25. Fabre, A. *et al.* Clinical Aspects of STAT3 Gain-of-Function Germline Mutations: A Systematic Review. *J. Allergy Clin. Immunol. Pract.* **7**, 1958-1969.e9 (2019).

26. Vogel, T. P., Milner, J. D. & Cooper, M. A. The Ying and Yang of STAT3 in Human Disease. *J. Clin. Immunol.* **35**, 615–623 (2015).

27. Lin, Q. *et al.* Constitutive Activation of JAK3/STAT3 in Colon Carcinoma Tumors and Cell Lines: Inhibition of JAK3/STAT3 Signaling Induces Apoptosis and Cell Cycle Arrest of Colon Carcinoma Cells. *Am. J. Pathol.* **167**, 969–980 (2005).

28. Lin, J. X. *et al.* The role of shared receptor motifs and common Stat proteins in the generation of cytokine pleiotropy and redundancy by IL-2, IL-4, IL-7, IL-13, and IL-15. *Immunity* **2**, 331–339 (1995).

29. JAK3 - Tyrosine-protein kinase JAK3 - Homo sapiens (Human) | UniProtKB | UniProt. https://www.uniprot.org/uniprotkb/P52333/entry#function.

30. Ghoreschi, K., Laurence, A. & O'Shea, J. J. Janus kinases in immune cell signaling. *Immunol. Rev.* **228**, 273–287 (2009).

31. Krolopp, J. E., Thornton, S. M. & Abbott, M. J. IL-15 Activates the Jak3/STAT3 Signaling Pathway to Mediate Glucose Uptake in Skeletal Muscle Cells. *Front. Physiol.* **7**, 626 (2016).

32. Liu, J. *et al.* JAK3/STAT3 oncogenic pathway and PRDM1 expression stratify clinicopathologic features of extranodal NK/T-cell lymphoma, nasal type. *Oncol. Rep.* **41**, 3219–3232 (2019).

33. Recent insights into targeting the IL-6 cytokine family in inflammatory diseases and cancer | Nature Reviews Immunology. https://www.nature.com/articles/s41577-018-0066-7.

34. Neuropoietin, a new IL-6-related cytokine signaling through the ciliary neurotrophic factor receptor | PNAS. https://www.pnas.org/doi/full/10.1073/pnas.0306178101.

35. Boeuf, H., Hauss, C., Graeve, F. D., Baran, N. & Kedinger, C. Leukemia Inhibitory Factor–dependent Transcriptional Activation in Embryonic Stem Cells. *J. Cell Biol.* **138**, 1207–1217 (1997).

36. Niwa, H., Burdon, T., Chambers, I. & Smith, A. Self-renewal of pluripotent embryonic stem cells is mediated via activation of STAT3. *Genes Dev.* **12**, 2048–2060 (1998).

37. Decker, T. & Kovarik, P. Serine phosphorylation of STATs. *Oncogene* **19**, 2628–2637 (2000).

38. Herrera, F., Chen, Q. & Schubert, D. Synergistic Effect of Retinoic Acid and Cytokines on the Regulation of Glial Fibrillary Acidic Protein Expression. *J. Biol. Chem.* **285**, 38915–38922 (2010).

39. Tolomeo, M. & Cascio, A. The Multifaced Role of STAT3 in Cancer and Its Implication for Anticancer Therapy. *Int. J. Mol. Sci.* **22**, 603 (2021).

40. Braunstein, J., Brutsaert, S., Olson, R. & Schindler, C. STATs Dimerize in the Absence of Phosphorylation *. *J. Biol. Chem.* **278**, 34133–34140 (2003).

41. Nkansah, E. *et al.* Observation of unphosphorylated STAT3 core protein binding to target dsDNA by PEMSA and X-ray crystallography. *FEBS Lett.* **587**, 833–839 (2013).

42. Yang, J. *et al.* Novel roles of unphosphorylated STAT3 in oncogenesis and transcriptional regulation. *Cancer Res.* **65**, 939–947 (2005).

43. Cornejo, M. G. *et al.* Constitutive JAK3 activation induces lymphoproliferative syndromes in murine bone marrow transplantation models. *Blood* **113**, 2746–2754 (2009).

44. Nairismägi, M.-L. *et al.* Oncogenic activation of JAK3-STAT signaling confers clinical sensitivity to PRN371, a novel selective and potent JAK3 inhibitor, in natural killer/T-cell lymphoma. *Leukemia* **32**, 1147–1156 (2018).

45. Li, S. D. *et al.* Cancer gene profiling in non-small cell lung cancers reveals activating mutations in JAK2 and JAK3 with therapeutic implications. *Genome Med.* **9**, 89 (2017).

46. Mittempergher, L. *et al.* Kinome capture sequencing of high-grade serous ovarian carcinoma reveals novel mutations in the JAK3 gene. *PLOS ONE* **15**, e0235766 (2020).

47. Smedley, W. & Patra, A. JAK3 Inhibition Regulates Stemness and Thereby Controls Glioblastoma Pathogenesis. *Cells* **12**, 2547 (2023).

48. Dammeijer, F. *et al.* Low-Dose JAK3 Inhibition Improves Antitumor T-Cell Immunity and Immunotherapy Efficacy. *Mol. Cancer Ther.* **21**, 1393–1405 (2022).

49. Cerami, E. *et al.* The cBio cancer genomics portal: an open platform for exploring multidimensional cancer genomics data. *Cancer Discov.* **2**, 401–404 (2012).

50. Garcia-Princival, I. M. R. *et al.* Streptomyces hygroscopicus UFPEDA 3370: A valuable source of the potent cytotoxic agent nigericin and its evaluation against human colorectal cancer cells. *Chem. Biol. Interact.* **333**, 109316 (2021).

51. Uckun, F. *et al.* Effect of Targeting Janus Kinase 3 on the Development of Intestinal Tumors in the Adenomatous Polyposis Colimin Mouse Model of Familial Adenomatous Polyposis. *Arzneimittelforschung* **57**, 320–329 (2011).

52. Mori, D., Nakafusa, Y., Miyazaki, K. & Tokunaga, O. Differential expression of Janus kinase 3 (JAK3), matrix metalloproteinase 13 (MMP13), heat shock protein 60 (HSP60), and mouse double minute 2 (MDM2) in human colorectal cancer progression using human cancer cDNA microarrays. *Pathol. - Res. Pract.* **201**, 777–789 (2005).

53. Diallo, M. & Herrera, F. The role of understudied post-translational modifications for the behavior and function of Signal Transducer and Activator of Transcription 3. *FEBS J.* **289**, 6235–6255 (2022).

54. Carpenter, R. L. & Lo, H.-W. STAT3 Target Genes Relevant to Human Cancers. *Cancers* **6**, 897–925 (2014).

55. Gordziel, C., Bratsch, J., Moriggl, R., Knösel, T. & Friedrich, K. Both STAT1 and STAT3 are favourable prognostic determinants in colorectal carcinoma. *Br. J. Cancer* **109**, 138–146 (2013).cCT

56. Corvinus, F. M. *et al.* Persistent STAT3 Activation in Colon Cancer Is Associated with Enhanced Cell Proliferation and Tumor Growth. *Neoplasia* **7**, 545–555 (2005).

57. Gargalionis, A. N., Papavassiliou, K. A. & Papavassiliou, A. G. Targeting STAT3 Signaling Pathway in Colorectal Cancer. *Biomedicines* **9**, 1016 (2021).

58. de Bruijn, I. *et al.* Analysis and Visualization of Longitudinal Genomic and Clinical Data from the AACR Project GENIE Biopharma Collaborative in cBioPortal. *Cancer Res.* **83**, 3861–3867 (2023).

59. Gao, J. *et al.* Integrative analysis of complex cancer genomics and clinical profiles using the cBioPortal. *Sci. Signal.* **6**, pl1 (2013).

60. Díez-Villanueva, A., Mallona, I. & Peinado, M. A. Wanderer, an interactive viewer to explore DNA methylation and gene expression data in human cancer. *Epigenetics Chromatin* **8**, 22 (2015).

61. Kõressaar, T. *et al.* Primer3_masker: integrating masking of template sequence with primer design software. *Bioinforma. Oxf. Engl.* **34**, 1937–1938 (2018).

62. Cloud-based platform for biotech R&D | Benchling. https://www.benchling.com.

63. CCDS Report for Consensus CDS. https://www.ncbi.nlm.nih.gov/CCDS/CcdsBrowse.cgi?REQUEST=GENEID&DATA=3718.

64. Christman, J. K. 5-Azacytidine and 5-aza-2′-deoxycytidine as inhibitors of DNA methylation: mechanistic studies and their implications for cancer therapy. *Oncogene* **21**, 5483–5495 (2002).

65. Schneider, C. A., Rasband, W. S. & Eliceiri, K. W. NIH Image to ImageJ: 25 years of image analysis. *Nat. Methods* **9**, 671–675 (2012).

66. Niu, B. *et al.* MSIsensor: microsatellite instability detection using paired tumor-normal sequence data. *Bioinforma. Oxf. Engl.* **30**, 1015–1016 (2014).

67. Jasmine, F. *et al.* Interaction between Microsatellite Instability (MSI) and Tumor DNA Methylation in the Pathogenesis of Colorectal Carcinoma. *Cancers* **13**, 4956 (2021).

68. Miranda, E. *et al.* Genetic and epigenetic changes in primary metastatic and nonmetastatic colorectal cancer. *Br. J. Cancer* **95**, 1101–1107 (2006).

69. Sondka, Z. *et al.* COSMIC: a curated database of somatic variants and clinical data for cancer. *Nucleic Acids Res.* **52**, D1210–D1217 (2024).

70. Multi-omics of 34 colorectal cancer cell lines - a resource for biomedical studies | Molecular Cancer | Full Text. https://molecular-cancer.biomedcentral.com/articles/10.1186/s12943-017-0691-y.

71. Cornejo, M. G., Boggon, T. J. & Mercher, T. JAK3: A two-faced player in hematological disorders. *Int. J. Biochem. Cell Biol.* **41**, 2376–2379 (2009).

72. He, Z., Song, B., Zhu, M. & Liu, J. Comprehensive pan-cancer analysis of STAT3 as a prognostic and immunological biomarker. *Sci. Rep.* **13**, 5069 (2023).

73. Fatemi, N. *et al.* DNA methylation biomarkers in colorectal cancer: Clinical applications for precision medicine. *Int. J. Cancer* **151**, 2068–2081 (2022).

74. Pathway Search Result. https://www.kegg.jp/kegg-bin/search_pathway_text?map=map&keyword=STAT3&mode=1&viewImage=true.

75. Long, Q. *et al.* Prognostic value of JAK3 promoter methylation and mRNA expression in clear cell renal cell carcinoma. *J. Adv. Res.* **40**, 153–166 (2022).

76. López, J. I. *et al.* A DNA hypermethylation profile reveals new potential biomarkers for the evaluation of prognosis in urothelial bladder cancer. *APMIS* **125**, 787–796 (2017).

77. Franzen, J. *et al.* DNA methylation changes during long-term in vitro cell culture are caused by epigenetic drift. *Commun. Biol.* **4**, 598 (2021).

78. Tost, J. & Gut, I. G. DNA methylation analysis by pyrosequencing. *Nat. Protoc.* **2**, 2265–2275 (2007).

79. Xiong, Z. & Laird, P. W. COBRA: a sensitive and quantitative DNA methylation assay. *Nucleic Acids Res.* **25**, 2532–2534 (1997).

80. Brooimans, R. A., Van Der Slot, A. J., Van Den Berg, A. J. & Zegers, B. J. Revised exon–intron structure of human JAK3 locus. *Eur. J. Hum. Genet.* **7**, 837–840 (1999).

81. Moghadasi, M. *et al.* Investigation the Cytotoxicity of 5-AZA on Acute Lymphoblastic Leukemia Cell Line In Vitro and Characterization the Underlying Molecular Mechanisms of Cell Death and Motility. *Asian Pac. J. Cancer Prev. APJCP* **22**, 3723–3734 (2021).

82. Epigenetic inactivation of the extracellular matrix metallopeptidase ADAMTS19 gene and the metastatic spread in colorectal cancer - PubMed. https://pubmed.ncbi.nlm.nih.gov/26634009/.

83. Verbsky, J. W. *et al.* Expression of Janus Kinase 3 in Human Endothelial and Other Non-lymphoid and Non-myeloid Cells*. *J. Biol. Chem.* **271**, 13976–13980 (1996).

84. Shareef, M. M., Shamloula, M. M., Elfert, A. A., El-sawaf, M. & Soliman, H. H. Expression of the signal transducer and activator of transcription factor 3 and Janus kinase 3 in colorectal carcinomas, colonic adenomas and ulcerative colitis. *Arab J. Gastroenterol.* **10**, 25–32 (2009).

85. Liu, R. *et al.* Methylation across the central dogma in health and diseases: new therapeutic strategies. *Signal Transduct. Target. Ther.* **8**, 1–46 (2023).

86. Haan, C. *et al.* Jak1 Has a Dominant Role over Jak3 in Signal Transduction through γc-Containing Cytokine Receptors. *Chem. Biol.* **18**, 314–323 (2011).

# VIII. Supplementary data

## A

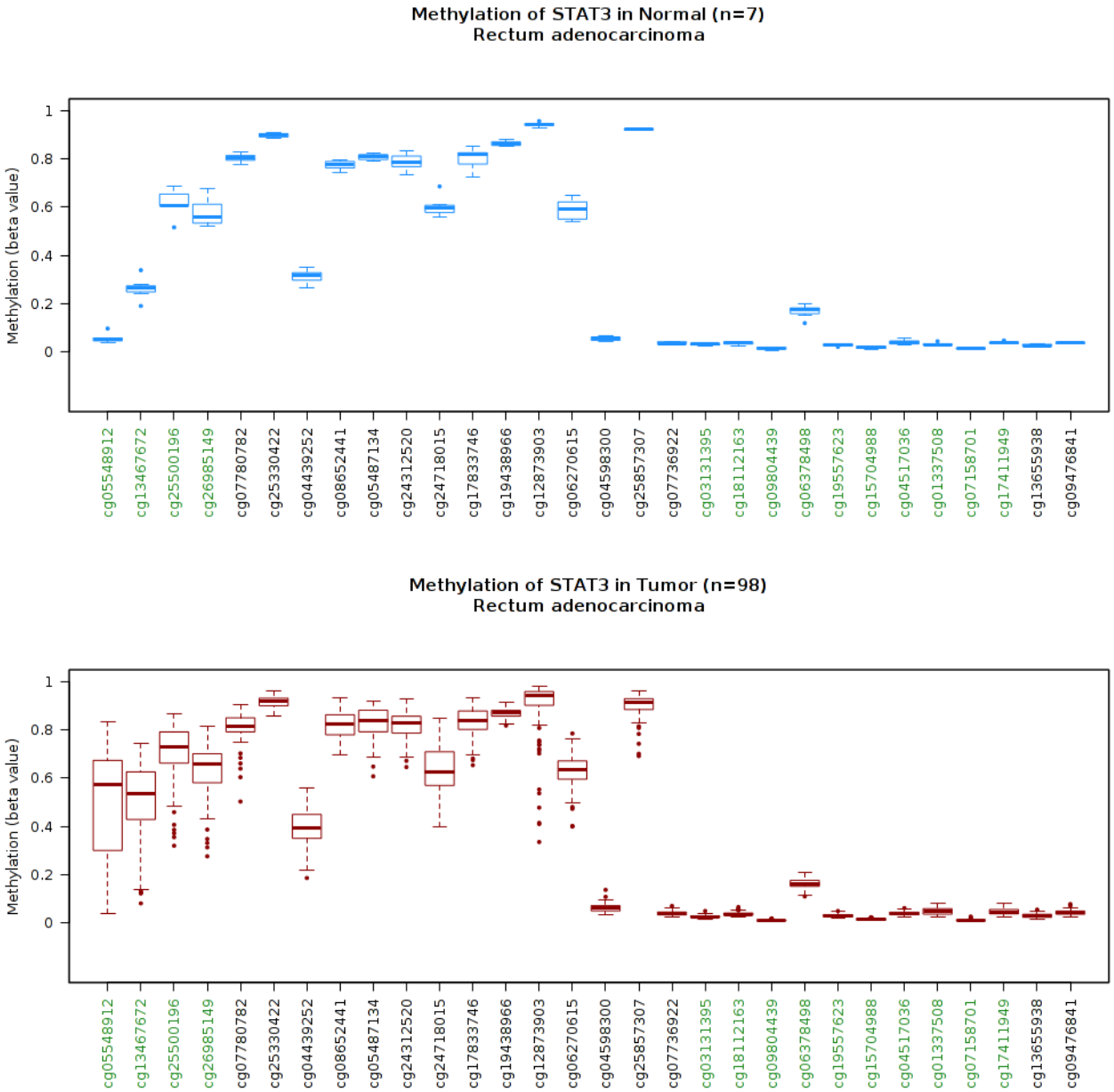

**B**

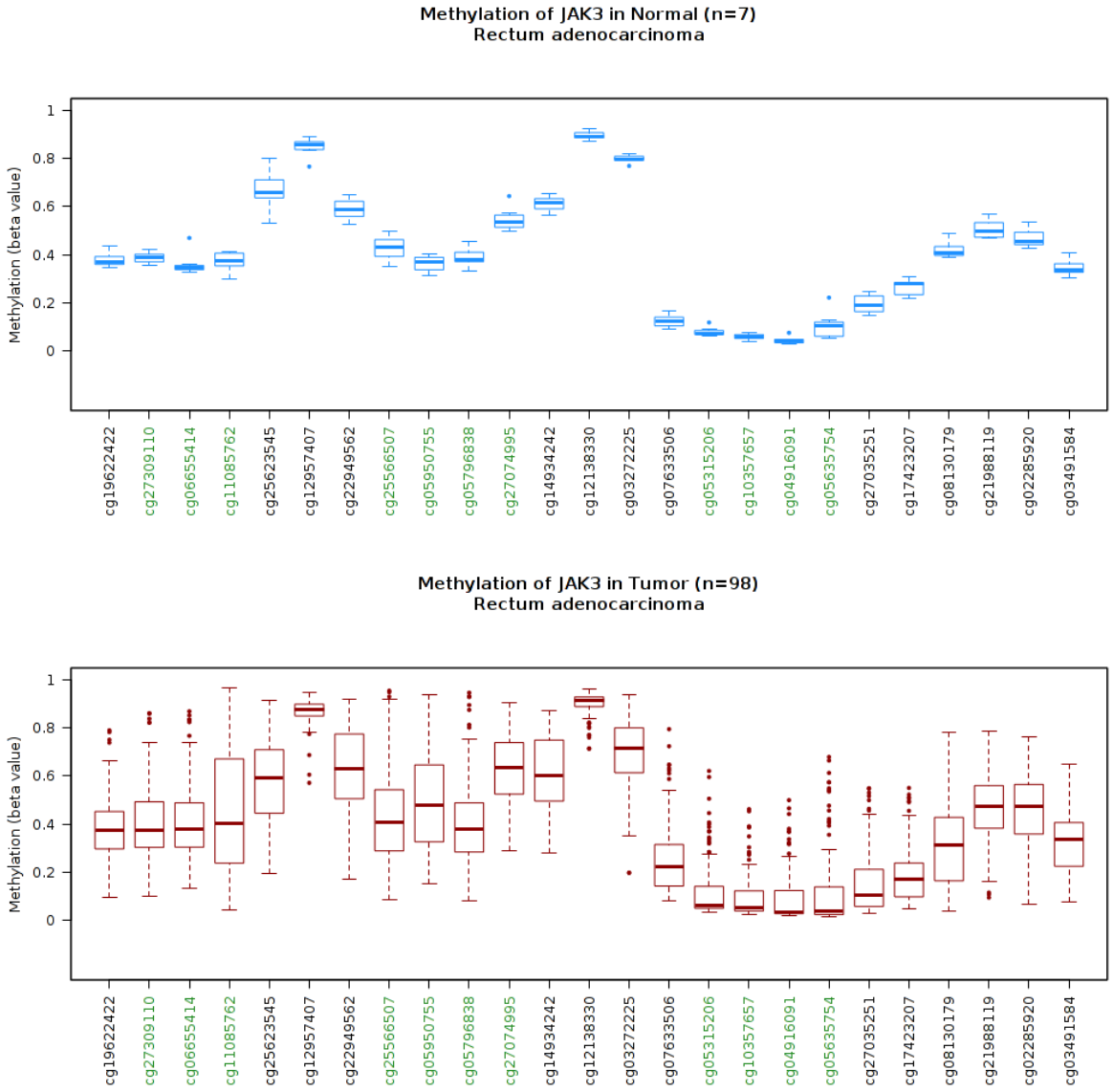


**Figure SD.1**- Methylation status of JAK3 and STAT3 in Rectum adenocarcinoma with the boxplot visualization, taken from TGCA wanderer. A- methylation status of STAT3; B- methylation status of JAK3